

UC San Diego

UC San Diego Previously Published Works

Title

Dihydropyridine Lactam Analogs Targeting BET Bromodomains.

Permalink

<https://escholarship.org/uc/item/2cs6g2cv>

Journal

ChemMedChem: chemistry enabling drug discovery, 17(1)

Authors

Jiang, Jiewei

Sigua, Logan

Chan, Alice

et al.

Publication Date

2022-01-05

DOI

10.1002/cmdc.202100407

Peer reviewed



Published in final edited form as:

ChemMedChem. 2022 January 05; 17(1): e202100407. doi:10.1002/cmdc.202100407.

Dihydropyridine Lactam Analogs targeting BET Bromodomains

Jiewei Jiang^a, Logan H. Sigua^b, Alice Chan^c, Prakriti Kalra^d, William C.K. Pomerantz^d, Ernst Schönbrunn^c, Jun Qi^{b,e}, Gunda I. Georg^a

^aDepartment of Medicinal Chemistry and Institute for Therapeutics Discovery and Development, College of Pharmacy, University of Minnesota, 717 Delaware Street, SE, Minneapolis, MN 55414

^bDepartment of Cancer Biology, Dana-Farber Cancer Institute, Boston, MA 02215

^cMoffitt Cancer Center, Drug Discovery Department, 12902 Magnolia Drive, Tampa, FL 33612

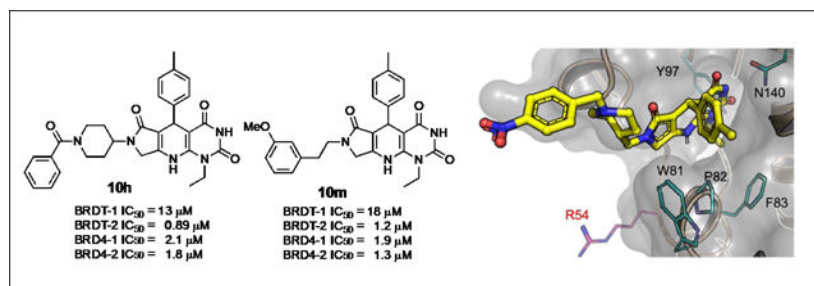
^dDepartment of Chemistry, University of Minnesota, Pleasant Street, SE, Minneapolis, MN 55455

^eDepartment of Medicine, Harvard Medical School, Boston, MA 02115

Abstract

Inhibitors of Bromodomain and Extra Terminal (BET) proteins are investigated for various therapeutic indications, but selectivity for BRD2, BRD3, BRD4, BRDT and their respective tandem bromodomains BD1 and BD2 remains suboptimal. Here we report selectivity-focused structural modifications of previously reported dihydropyridine lactam **6** by changing linker length and linker type of the lactam side chain in efforts to engage the unique arginine 54 (R54) residue in BRDT-BD1 to achieve BRDT-selective affinity. We found that the analogs were highly selective for BET bromodomains, and generally more selective for the first (BD1) and second (BD2) bromodomains of BRD4 rather than for those of BRDT. Based on AlphaScreen and BromoScan results and on crystallographic data for analog **10j**, we concluded that the lack of selectivity for BRDT is most likely due to the high flexibility of the protein and the unfavorable trajectory of the lactam side chain that do not allow interaction with R54. A 15-fold preference for BD2 over BD1 in BRDT was observed for analogs **10h** and **10m**, which was supported by protein-based ¹⁹F NMR experiments with a BRDT tandem bromodomain protein construct.

Graphical Abstract



Introduction

Acetylation of ε-N-lysine residues on histone tails has been recognized as an important post-translational modification¹⁻⁴ that neutralizes the positively charged lysine thereby

reducing affinity for the negatively charged DNA in the nucleosome, a process that makes DNA accessible for the transcriptional machinery.⁵⁻⁸ During this process, BET bromodomains bind to the acetylated lysine (KAc) motif and recruit other proteins such as positive transcription elongation factor B (P-TEFb) and RNA polymerase II (Pol II) to initiate gene transcription.⁹ Recent studies have shown that the bromodomain-containing protein family is involved in both normal and disease-related epigenetic processes.¹⁰⁻¹² Among the eight bromodomain families, the bromodomain and extra terminal (BET) subfamily has been studied most extensively.³ The BET proteins BRD2, BRD3, BRD4 are ubiquitously expressed, whereas BRDT is restricted to the testis.¹³ Each protein contains two tandem bromodomains referred to as BD1 and BD2. BRDT has been validated genetically and pharmacologically as a target for male contraception. BRDT-1 (BD1 of BRDT) alone and BRDT-1/BRDT-2 (BD1 and BD2 of BRDT) double knock-out male mice are healthy but infertile.¹³⁻¹⁶ Inhibition of BRDT with the pan-BET inhibitor (+)-JQ1 led to reversible infertility in mice.¹⁷ However, (+)-JQ1 is not suitable for development as a male contraceptive agent because it has higher affinity for BRD4 than BRDT and has a short half-life.¹⁷⁻¹⁸ In addition to the well-known tool compound (+)-JQ1,¹⁹ various scaffolds have been reported as potent BET inhibitors by both industrial and academic laboratories (Figure 1).²⁰⁻²³

Many of the reported BET inhibitors displaying excellent potencies share a similar binding mode with BET proteins. As exemplified by (+)-JQ1, inhibitors competitively occupy the KAc binding site of histones via a key hydrogen bond with a conserved asparagine (N109 of BRDT-1, Figure 2A), and have hydrophobic contacts with the WPF shelf (W50, P51, and F52 of BRDT-1, Figure 2A). According to the sequence comparison, the highly conserved nature of the KAc sites in all BET bromodomains results in the low intra/inter-BET selectivity of most reported molecules. The lack of selective inhibitors has made it challenging to investigate the individual functions of the BET bromodomains and can lead to unwanted off-target effects.²⁴ For instance, molibresib (GSK525762, **1b**, Figure 1) displayed significant side effects that led to dose interruption and treatment discontinuation in a phase I/II study for the treatment of advanced solid tumors.²⁵ Thus, the motivation to develop isoform and bromodomain-selective inhibitors is compelling. Some success has been achieved.^{8, 26-27} ABBV-744 (**2**, Figure 1)²⁸ is in clinical trials for myeloid leukemia and prostate cancer, apabetalone (RVX-208, **4**, Figure 1),²² has received FDA Breakthrough Therapy Designation for the treatment of cardiovascular disease, and GSK046 (**3a**) is effective in animal models of inflammation and autoimmune disease.²⁹ All of them bind with higher affinity to the BD2 bromodomains than to the BD1 bromodomains of the BET bromodomain family members. Recently a BD2 selective inhibitor CDD-1349 (**5**, Figure 1) with 6-fold selectivity for BRDT-BD2 (IC₅₀ = 22 nM) over BRD4-BD2 (IC₅₀ = 140 nM) and excellent stability against human liver microsomes was reported.¹⁸ A highly BD1-selective anticancer agent, GSK778 (**3b**), has also been discovered recently.²⁹ Furthermore, Tanaka et al. reported a series of (+)-JQ1-derived dimeric analogs, including MT1, which displays excellent BRD4 selectivity by intramolecular bivalent binding to BRD4-1 and BRD4-2.³⁰

Another possibility to attain selectivity could come from leveraging the differences in the amino acid residues in different BET bromodomains such as the unique positively charged

R54 in human BRDT-1 at the entrance to the ZA channel (Figure 2B). The other three BET BD1 bromodomains have a neutral glutamine in this position. Another difference is the presence of an asparagine (N297) in BRDT-2 where the other BD2s have a lysine residue in the equivalent position (Figure 2C). It is not currently known whether the single knock-out of BRDT-2 will induce male infertility. However, given its essential role in post-meiotic sperm differentiation by promoting the histone to protamine reorganization that is needed for the packaging of the genome into the nucleus of spermatozoa, an effect on male fertility is likely.^{31–32} Thus, a highly selective BRDT-2 inhibitor could potentially be developed into a male contraceptive agent. We hypothesized that selectivity for BRDT-1 might be achieved by engaging R54. Arginine can either form ionic interaction with negatively charged residues with covalent-like bond strength,^{34–35} form cation- π interactions^{36–38} with electron-rich ring systems, or form hydrophobic interactions with non-polar aromatic and aliphatic side chains above and below the guanidinium plane.³⁹

We recently reported the synthesis and evaluation of dihydropyridines, including lactam analogs **6a** and **6b** (Figure 1) for BET affinity.²³ In comparison with the corresponding lactones, the lactam analogs **6** showed increased affinities. We also had established that the N1-ethyl group is optimal for this scaffold by occupying a lipophilic pocket of the bromodomains that is surrounded by conserved water molecules. Furthermore, the dihydropyridine is essential for affinity since the corresponding pyridines are inactive. Previously we had found that the 5-tolyl group, which is interacting with the lipophilic WPF shelf formed by W50/P51/F52 in the histone binding site, as an optimal group for BRDT-1 and BRD4-1 affinity.²³ Keeping these structural elements in place, we investigated whether modifications of the lactam side chain could improve BET affinity and selectivity by inducing interactions with R54 of BRDT-1. For the design of the lactam side chain modifications, we pursued two approaches, probing the linker region, which determines side chain orientation, and investigating the effects of different functional groups attached to the linker to tune interactions with additional residues of the BET proteins.

Results and Discussions

The initial method to prepare the targeted lactam analogs is illustrated in Scheme 1. Ethyl urea and ethyl cyanoacetoacetate were first converted to 6-amino-1-ethylpyrimidine-2,4(1*H*,3*H*)-dione (**7**), employing sodium *tert*-butoxide as the base. Knoevenagel condensation between ethyl chloroacetoacetate and *p*-tolylaldehyde generated the other key intermediate **8** as a mixture of E/Z isomers. The Hantzsch dihydropyridine synthesis was then used to construct bicyclic intermediate **9** by reacting intermediates **7** and **8** in methanol in the presence of magnesium sulfate. A microwave-assisted reaction of intermediate **9** with primary amines generated the targeted lactam analogs **10**.

We realized that the low yielding dihydropyridine synthesis step would make it challenging to efficiently prepare analogs. Therefore, we sought to pinpoint the causes for the low yield of this reaction. One reason for the low yield was the limited solubility of intermediate **7** in methanol. We also noted an impurity that consistently co-eluted with desired compound **9** during the purification. According to the proton NMR of this mixture, we speculated that the impurity could be a regioisomer of **9**. Based on the proposed reaction mechanism,

dehydration of the hydroxyl intermediate (black box, Scheme 2) can take place at two different sites (indicated by the blue and red dots, Scheme 2), which generates the desired dihydropyridine **9** and regioisomer **9'**. The similar polarity of **9'** and **9** stymied the isolation and therefore diminished the yield.

Taking these results into consideration, we designed the new route shown in Scheme 3, in which the chlorine was introduced in the penultimate step of the reaction sequence so that the undesired dehydration is no longer possible. The reaction between ethyl 4-chloro-3-oxobutanoate and benzyl alcohol furnished benzyl ether **11**, which was subjected to a Knoevenagel condensation to form intermediate **12**. Next, intermediate **12** and *N*-ethyluracil **7** were completely dissolved in acetic acid under the reflux conditions, which provided Hantzsch reaction product **13** in 42% yield. The increased solubility of uracil **7** in acetic acid and prevention of regioisomer formation contributed to achieving a better yield than with the previous method. A boron tribromide solution was used to cleave the ether bond and generate hydroxyl intermediate **14**, which was converted into key chloromethyl intermediate **9** using sulfuryl chloride and imidazole. Despite an increase in the number of chemical steps, the optimized route simplified product purification and increased the overall yield.

We initially prepared ten lactam analogs (**10a** – **10j**) with linear or cyclic linkers of varying lengths and tested them for BRDT and BRD4 affinity using BRDT-1, BRDT-2, BRD4-1, and BRD4-2 to characterize their selectivity profiles using AlphaScreen assays (Table 1).

Analogs carrying either an *N*-allyl (**10a**) or an *N*-benzyl group (**10b**) displayed similar activities against the four BET constructs. Comparison of analog **10b**, **10c**, and **10d** revealed that a longer, linear, and more flexible linker reduced affinity, presumably because of an entropic penalty. This reduction of affinity was most significant against BRDT-1, with a more than 5-fold decrease from **10b** to **10d**. Notably, the introduction of an oxygen atom into the linker (**10e**) rescued affinity to some degree. Although it improved water solubility, a piperidine linker had little effect on affinity (compounds **10f** – **10i**). Collectively, either linear or cyclic linker moieties had marginal impact on BRDT-1 selectivity. From an intra-BET perspective, all analogs displayed similar affinities against the BD1 and BD2 constructs in BRD4. Whereas in BRDT, analogs **10d**, **10e**, and **10h** showed up to 15-fold BD2 selectivity over BD1.

We then investigated the substitution effect on the aryl ring, using **10c** as the template, envisioning that an electron-rich aromatic ring could engage in a cation- π interaction with the unique R54 in BRDT-1. The results (Table 2), however, suggested that collectively, aromatic substitution had no significant effect on affinity. Analogs with electron-donating groups (**10k**, **6a**, and **6b**) were slightly more potent than analog **10l** with an electron-withdrawing group. A methoxy scan on the aryl ring (**6b**, **10m**, and **10n**) revealed that the 4-methoxy analog **6b** produced the best results, followed by 2-methoxy and 3-methoxy substitution. Disubstitution with methoxy or chlorine moieties (**10o**, **10p**, and **10q**) failed to show any improvement of BET activity and 3,4-dimethoxy analog **10o** experienced the greatest loss of affinity against BRDT-1. With respect to selectivity, none of the aryl modifications had significant impact on BRDT-1 specificity. Furthermore, this subset of analogs showed similar activities for BRD4-1 and BRD4-2. Meanwhile, there was a BD2

preference over BD1 in BRDT among all the analogs, especially analog **10m** with 15-fold BRDT-2 selectivity.

To further assess the selectivity of our two inhibitors **10h** and **10m**, we used a new protein-observed fluorine (PrOF) NMR experiment. In this experiment, the tandem bromodomains of BRDT are 5-fluorotryptophan (5FW)-labeled, (5FW BRDT-T) including the WPF shelf tryptophans in BD1 and BD2, W50 and W293 respectively.⁴⁰ Figure 3 shows the PrOF NMR titration of **10h** and **10m** with 5FW BRDT-T. For both **10h** and **10m** at near stoichiometric concentrations of inhibitor (26 μM of **10h** and 31 μM of **10m**) the W293 ¹⁹F resonance for BD2 is in intermediate chemical exchange and broadens into the baseline, whereas the W50 BD1 ¹⁹F resonance is less significantly perturbed until BD2 is fully bound. This result is consistent with our AlphaScreen data showing an approximate 15-fold selectivity for BD2 over BD1 for the two inhibitors. The response of the W293 BD2 ¹⁹F resonance is in intermediate chemical exchange, an exchange regime consistent with $\sim 1 \mu\text{M}$ IC₅₀ values. Together, these results support **10h** and **10m** interacting with the WPF shelf near the histone binding site, with affinities and selectivity comparable to those measured by AlphaScreen on isolated domains.

To test for selectivity against other bromodomains, compound **10m** was tested in a selectivity screen against a panel of 33 bromodomains in a bromodomain qPCR-based bromodomain displacement assay (Figure 4) at 20 μM concentration (BromoScan, Eurofins). Compound **10m** was found to be highly selective for the BET bromodomain family. Only Cat eye syndrome critical region protein 2 (CECR2) was slightly inhibited (28% remaining at 10 μM).

Analog **10c** could be co-crystallized with BRD4-1, however, the complex only had acceptable resolution for the dihydropyridine core in the binding site. The phenethyl side chain showed poorly defined electron density, indicating that the lactam side chain was rather flexible. Such flexibility could decrease the possibility for any interaction between R54 and the lactam side chain and is the likely cause for the lack of the desired BRDT-1 selectivity among the synthesized analogs.

We next embarked on the introduction of a carboxylic acid in the side chain, seeking to form an ionic interaction with R54 to increase BRDT-1 selectivity. To this end, we designed and prepared five carboxylic acid analogs (**10r** – **10v**) with varied linker length of 6–12 atoms attached to the lactam nitrogen.

As shown in Table 3, a comparison of these analog with related ones lacking the carboxylic acid moiety (Table 1) revealed that the carboxylate motif had marginal effect on BRDT-1 affinity and selectivity. We speculate that the orientation of the lactam side chain must not be optimal to engage R54 in BRDT-1.

We were able to obtain a co-crystal structure of BRD4-1 with **10j**, a compound with a conformationally constrained side chain. Nevertheless, we observed that the nitrobenzene moiety reaches into the solvent exposed area (Figure 5). The ionic interaction with R54 requires a head-to-head orientation with the negatively charged group, which would necessitate conformational changes of the protein or the ligand to allow interaction between

the analog and the target R54. Such movement of the protein could be challenging especially in the solvent exposed environment of R54 and because R54 is among the most flexible residues in crystal structures of BRDT.

Conclusions

In this study, we explored structural changes in the dihydropyridine lactam side chain of analog **6** to investigate its impact on both BET affinity and selectivity. Multiple side chain modifications were carried out, but they did not improve BET affinity or selectivity among the BET proteins. We also failed in engaging the unique R54 in BRDT-1 although we tuned the electronegativity of the aryl ring for cation- π interaction and introduced a carboxylate for ionic interaction. All analogs showed a slight preference for BRD4-1 over BRDT-1, including analogs **10h** and **10m**. However, these two analogs exhibited a 15-fold preference for BD2 over BD1 in BRDT. This BD2 selectivity was confirmed with a PrOF NMR experiment using 5FW BRDT-T. A BromoScan against a panel of 33 bromodomains showed that **10m** was highly selective for BET bromodomains. Based on the AlphaScreen assay results and the crystallographic data, we reasoned that the lack of BRDT-1 selectivity was a result of the lactam side chain flexibility and the suboptimal orientation of the lactam side chain observed in the crystal structure of compound **10j**. Furthermore, R54 is among the most flexible residues in crystal structures of BRDT, which may have prevented interaction of the analogs with the R54 residue. Another issue could relate to a penalty encountered for desolvating the interacting groups, which could be higher or similar to the enthalpy gained from the interactions between the protein and the small molecule. Either a different chemical scaffold that can achieve the desired trajectory and interaction with R54 or other strategies such as targeting N-297 will be needed to achieve BRDT selectivity. Analog **10h** and **10m** could be considered as starting points for future medicinal chemistry optimizations to obtain BRDT-2 selective inhibitors.

Experimental Section

Chemistry

General: All chemicals and solvents were purchased from commercial suppliers and directly used without further purification unless otherwise specified. Reactions performed under microwave irradiation used the Biotage Initiator. Reactions were monitored by TLC on 0.2 mm silica gel plates (Merck Kieselgel GF254) and visualized under UV light (254 nm). Preparatory-scale flash column chromatography was conducted using medium-pressure liquid chromatography (MPLC) on a CombiFlash[®] Companion (Teledyne ISCO) with pre-packed silica columns (20 – 40 microns) and UV detection at 254 nm. ¹H and ¹³C NMR spectra were performed on a Bruker 400/100 MHz Avance DPX. Chemical shifts were reported in parts per million (ppm) and coupling constants (*J*). Splitting patterns were designed as s, singlet; d, doublet; t, triplet; q, quartet; m, multiplet; br s, broad singlet. Melting points are uncorrected. Purities of tested compounds were determined either by UPLC or qNMR, using DMSO₂ as the internal standard and the qNMR protocol published in the *Journal of Medicinal Chemistry*.^{41–42}

6-Amino-1-ethylpyrimidine-2,4(1*H*,3*H*)-dione (7).

Based on a reported procedure,⁴³ ethyl 2-cyanoacetate (12.8 g, 113.5 mmol) and 1-ethylurea (10.0 g, 113.5 mmol) were dissolved in anhydrous ethanol (250 mL) in a 500-mL round-bottomed flask. Sodium *tert*-butoxide (21.8 g, 227.0 mmol) was then added and the mixture was stirred under reflux conditions for 24 h. After cooling to rt, the solvent was evaporated under reduced pressure, and the residue was dissolved in distilled water (100 mL). The pH of the solution was adjusted to 1 – 2 with a 1M HCl solution. The solid formed was collected by filtration, washed with water, and dried under reduced pressure to afford the title compound as a brown solid (16.0 g, 91%). ¹H NMR (400 MHz, DMSO-*d*₆) δ 10.26 (s, 1H), 6.77 (s, 2H), 4.51 (s, 1H), 3.76 (q, *J* = 7.0 Hz, 2H), 1.07 (t, *J* = 7.0 Hz, 3H).

Ethyl 4-Chloro-2-(4-methylbenzylidene)-3-oxobutanoate (8).

Ethyl 4-chloro-3-oxobutanoate (1.5 g, 9.1 mmol) and *p*-tolualdehyde (1.0 g, 8.7 mmol) were dissolved in ethanol (100 mL). Piperidine (74 mg, 0.87 mmol) and acetic acid (52 mg, 0.87 mmol) were added. The resulting solution was stirred at rt for 24 h. The solvent was evaporated under reduced pressure, poured into water, and extracted with EtOAc. The organic phase was washed with brine, dried over anhydrous MgSO₄, and concentrated under reduced pressure. The residue was further purified by flash column chromatography (40 g RediSep Gold silica gel column, 0 – 5% EtOAc in hexanes) to yield a yellow viscous oil as a ~3:1 *E/Z* isomer mixture (1.3 g, 57%). ¹H NMR (400 MHz, CDCl₃) δ 7.81 (s, 0.77H), 7.73 (s, 0.26H), 7.37 (d, 7.5 Hz, 0.6H), 7.35 – 7.18 (m, 3.4H), 4.36 – 4.20 (m, 4H), 2.37 (3H), 1.35 – 1.23 (m, 3H).

Ethyl 7-(Chloromethyl)-1-ethyl-2,4-dioxo-5-(*p*-tolyl)-1,2,3,4,5,8-hexahydropyrido[2,3-*d*]pyrimidine-6-carboxylate (9).

A solution of sulfonyl chloride (0.62 mL, 7.7 mmol) in DMF (5 mL) was added dropwise over 5 min to a stirred, ice-cooled solution of ethyl 1-ethyl-7-(hydroxymethyl)-2,4-dioxo-5-(*p*-tolyl)-1,2,3,4,5,8-hexahydropyrido[2,3-*d*]pyrimidine-6-carboxylate (1.5 g, 3.8 mmol) and imidazole (0.68 g, 10 mmol) in DMF (20 mL). After the removal of the ice bath, the mixture was stirred at rt for 0.5 h, diluted with EtOAc, washed with water, and dried over anhydrous MgSO₄. The solvent was removed under reduced pressure and the residue was purified by flash column chromatography (40 g RediSep Gold silica gel column, DCM + 2.0% methanol) to yield the title compound as a light-yellow solid (0.87 g, 56%); mp 266 – 267 °C dec; 96% purity determined by UPLC. ¹H NMR (400 MHz, DMSO-*d*₆) δ 11.03 (s, 1H), 8.99 (s, 1H), 7.07 (d, *J* = 8.0 Hz, 2H), 7.02 (d, *J* = 8.0 Hz, 2H), 5.17 (AB_q, *J* = 11.0 Hz, 1H), 4.88 (s, 1H), 4.72 (AB_q, *J* = 11.0 Hz, 1H), 4.07 (m, 3H), 3.96 – 3.86 (m, 1H), 2.20 (s, 3H), 1.20 – 1.11 (m, 6H). ¹³C NMR (100 MHz, DMSO-*d*₆) δ 165.2, 161.3, 149.8, 144.0, 143.2, 142.7, 135.5, 128.7, 127.1, 107.1, 89.7, 60.2, 48.6, 36.4, 35.7, 20.6, 13.9, 13.5. HRMS: calcd for C₂₀H₂₂ClN₃NaO₄ [M + Na]⁺, 426.1191; found 426.1199.

Ethyl 4-(Benzyloxy)-3-oxobutanoate (11).

To a suspension of sodium hydride (60% dispersion in mineral oil, 6.5 g, 162.8 mmol) in THF (100 mL) at 0 °C was added benzyl alcohol (8.4 g, 77.7 mmol) dropwise. The mixture was stirred at rt for 2 h. To this mixture was then added ethyl 4-chloroacetoacetate (12.2

g, 74.0 mmol) dropwise over 30 min. The resulting dark orange mixture was further stirred at rt overnight before it was cooled to 5 °C, acidified to pH ~4 using 1M HCl solution and extracted with EtOAc. The organic phase was washed with brine, dried over anhydrous MgSO₄, and concentrated under reduced pressure. The residue was then purified by flash column chromatography (40 g RediSep Gold silica gel column, 0 – 10% EtOAc in hexanes) to give the title compound as light-yellow viscous oil (12.7 g, 73%). ¹H NMR (400 MHz, CDCl₃) δ 7.37 – 7.33 (m, 5H), 4.59 (s, 2H), 4.18 (q, *J* = 7.1 Hz, 2H), 4.14 (s, 2H), 3.54 (s, 2H), 1.25 (t, *J* = 7.1 Hz, 3H).

Ethyl 4-(Benzyloxy)-2-(4-methylbenzylidene)-3-oxobutanoate (12).

Ethyl 4-(benzyloxy)-3-oxobutanoate (12.7 g, 53.9 mmol) and *p*-tolualdehyde (6.5 g, 53.9 mmol) were dissolved in ethanol (100 mL). Piperidine (0.46 g, 5.4 mmol), and acetic acid (0.32 g, 5.4 mmol) were added. The resulting solution was stirred at rt for 24 h. The solvent was evaporated under reduced pressure, poured into water, and extracted with EtOAc. The organic phase was washed with brine, dried over anhydrous MgSO₄, and concentrated under reduced pressure. The residue was further purified by flash column chromatography (40 g RediSep Gold silica gel column, 0 – 10% EtOAc in hexanes) to yield a yellow viscous oil in a ~4:1 ratio of *E/Z* isomers (8.1 g, 56%). ¹H NMR (400 MHz, CDCl₃) δ 7.76 (s, 0.8H), 7.70 (s, 0.2H), 7.36 – 7.34 (m, 3H), 7.30 (d, *J* = 6.8 Hz, 6H), 7.17 (t, *J* = 7.9 Hz, 2H), 4.60 (s, 0.8H), 4.59 (s, 0.2H), 4.25 – 4.07 (m, 2H), 4.27 (s, 2H), 2.37 (s, 0.6H), 2.36 (s, 2.4H), 1.27 (t, *J* = 7.3 Hz, 2.4H), 1.2 (t, *J* = 7.3 Hz, 0.6H).

Ethyl 7-((Benzyloxy)methyl)-1-ethyl-2,4-dioxo-5-(*p*-tolyl)-1,2,3,4,5,8-hexahydropyrido[2,3-*d*]pyrimidine-6-carboxylate (13).

4-(Benzyloxy)-2-(4-methylbenzylidene)-3-oxobutanoate (12.7 g, 37.5 mmol) and 6-amino-1-ethylpyrimidine-2,4(1*H*,3*H*)-dione (5.8 g, 37.5 mmol) were added into a 250-mL round-bottomed flask followed by the addition of acetic acid (100 mL). The mixture was heated to reflux overnight, during which the reaction turned into a clear light brown solution. After cooling to rt, acetic acid was removed under reduced pressure. Saturated NaHCO₃ solution (150 mL) was charged into the flask portion-wise and the mixture was allowed to stir for additional 0.5 h to neutralize the residual acid. A yellow solid precipitated from the aqueous solution and was collected by filtration. The solid was further washed with hexanes and water twice. After drying under reduced pressure, the crude title compound (12.7 g, 71%) was used for the next step without further purification. ¹H NMR (400 MHz, DMSO-*d*₆) δ 10.98 (s, 1H), 8.46 (s, 1H), 7.40 – 7.26 (m, 5H), 7.08 (d, *J* = 7.6 Hz, 2H), 7.01 (d, *J* = 7.7 Hz, 2H), 4.97 (AB_q, *J* = 14.0 Hz, 1H), 4.88 (s, 1H), 4.59 (AB_q, *J* = 14.0 Hz, 1H), 4.58 (s, 2H), 4.07 – 3.96 (m, 3H), 3.94 – 3.79 (m, 1H), 2.20 (s, 3H), 1.12 (t, *J* = 7.1 Hz, 3H), 1.07 (t, *J* = 6.9 Hz, 3H). ¹³C NMR (100 MHz, DMSO-*d*₆) δ 165.8, 161.3, 149.8, 143.8, 143.7, 143.1, 137.7, 135.3, 128.6, 128.2, 127.69, 127.65, 127.1, 105.3, 89.7, 71.9, 65.5, 59.8, 36.1, 35.9, 20.5, 14.0, 13.2.

Ethyl 1-Ethyl-7-(hydroxymethyl)-2,4-dioxo-5-(*p*-tolyl)-1,2,3,4,5,8-hexahydropyrido[2,3-*d*]pyrimidine-6-carboxylate (14).

Ethyl 7-((benzyloxy)methyl)-1-ethyl-2,4-dioxo-5-(*p*-tolyl)-1,2,3,4,5,8-hexahydropyrido[2,3-*d*]pyrimidine-6-carboxylate (2.8 g, 6.0 mmol) was dissolved in anhydrous DCM (50 mL)

in a two-necked round-bottomed flask (250 mL) equipped with a nitrogen balloon and a septum. The resulting yellow solution was cooled to $-78\text{ }^{\circ}\text{C}$ before the addition of boron tribromide (1 M solution, 18 mL, 18 mmol) dropwise. The solution was stirred for an additional 0.5 h after the removal of the dry ice bath. After total consumption of the starting material as monitored by TLC, the reaction was quenched by the addition of methanol and a saturated NaHCO_3 solution. The mixture was extracted with EtOAc and the organic phase was washed with brine, dried over anhydrous MgSO_4 , and concentrated under reduced pressure. The residue was then purified by flash column chromatography (40 g RediSep Gold silica gel column, DCM + 5.0% methanol) to yield the title compound as a white solid (1.5 g, 64%). ^1H NMR (400 MHz, $\text{DMSO}-d_6$) δ 10.99 (s, 1H), 8.36 (s, 1H), 7.08 (d, $J = 7.9$ Hz, 2H), 7.01 (d, $J = 7.9$ Hz, 2H), 5.99 (t, $J = 4$ Hz, 1H), 4.86 (s, 1H), 4.79 (AB_q, dd, $J = 16.3, 4.6$ Hz, 1H), 4.55 (AB_q, dd, $J = 16.3, 4.9$ Hz, 1H), 4.07 – 4.01 (m, 3H), 3.96 – 3.81 (m, 1H), 2.20 (s, 3H), 1.16 (dt, $J = 16.0, 7.0$ Hz, 6H). ^{13}C NMR (100 MHz, $\text{DMSO}-d_6$) δ 165.8, 161.3, 149.8, 147.2, 143.6, 143.4, 135.2, 128.5, 127.1, 101.9, 89.2, 59.5, 58.3, 36.1, 35.9, 20.5, 14.1, 13.2.

General Procedure for the synthesis of Lactam Analogs

Chloromethyl intermediate **9** (1 equiv) and the corresponding primary amine (1.1 equiv) were charged into a dry microwave tube (2 mL). After addition of ethanol (1 mL), the tube was flushed with nitrogen gas and capped. The reaction was heated to $120\text{ }^{\circ}\text{C}$ for 30 s in the microwave reactor, which gave rise to a dark orange solution. The mixture was subsequently loaded on a cartridge and purified by flash column chromatography (4 g RediSep Gold silica gel column, DCM + 10% methanol) to yield the desired compound.

7-Allyl-1-ethyl-5-(*p*-tolyl)-5,7,8,9-tetrahydro-1*H*-pyrrolo[3',4':5,6]pyrido[2,3-*d*]pyrimidine-2,4,6(3*H*)-trione (10a).

The title compound was prepared using the general procedure for the synthesis of the lactam analogs using chloromethyl intermediate **9** (50 mg, 0.12 mmol) and allylamine (7.8 mg, 0.14 mmol), which yielded a yellow solid (14 mg, 31%); mp $246 - 247\text{ }^{\circ}\text{C}$ dec; 93% purity determined by UPLC. ^1H NMR (400 MHz, $\text{DMSO}-d_6$) δ 10.39 (s, 1H), 8.89 (s, 1H), 7.15 (d, $J = 7.9$ Hz, 2H), 7.00 (d, $J = 7.8$ Hz, 2H), 5.83 – 5.74 (m, 1H), 5.28 (AB_q, $J = 16.6$ Hz, 1H), 5.09 (AB_q, $J = 16.6$ Hz, 1H), 5.04 (d, $J = 19.1$ Hz, 1H), 4.93 (d, $J = 19.1$ Hz, 1H), 4.89 (s, 1H), 4.01 (q, $J = 6.8$ Hz, 2H), 3.86 (s, 2H), 2.20 (s, 3H), 1.09 (t, $J = 6.8$ Hz, 3H). ^{13}C NMR (100 MHz, $\text{DMSO}-d_6$) δ 175.4, 172.8, 162.0, 155.3, 150.9, 143.7, 134.8, 133.6, 128.3, 127.1, 115.9, 93.4, 90.0, 75.1, 43.3, 35.7, 32.3, 20.6, 14.0. HRMS: calcd for $\text{C}_{21}\text{H}_{23}\text{N}_4\text{O}_3$ $[\text{M} + \text{H}]^+$, 379.1765; found 379.1771.

7-Benzyl-1-ethyl-5-(*p*-tolyl)-5,7,8,9-tetrahydro-1*H*-pyrrolo[3',4':5,6]pyrido[2,3-*d*]pyrimidine-2,4,6(3*H*)-trione (10b).

The title compound was synthesized via the general procedure for the lactam analogs using chloromethyl intermediate **9** (50 mg, 0.12 mmol) and benzylamine (15 mg, 0.14 mmol), which yielded a yellow solid (18 mg, 35%); mp $223 - 224\text{ }^{\circ}\text{C}$ dec; 97% purity determined by UPLC. ^1H NMR (400 MHz, $\text{DMSO}-d_6$) δ 10.40 (s, 1H), 9.18 (s, 1H), 7.31 – 7.21 (m, 3H), 7.17 (d, $J = 7.9$ Hz, 2H), 7.08 (d, $J = 6.1$ Hz, 2H), 7.02 (d, $J = 7.9$ Hz, 2H), 5.28 (AB_q, J

= 16.6 Hz, 1H), 5.12 (AB_q, J = 16.6 Hz, 1H), 4.91 (s, 1H), 4.45 (d, J = 5.7 Hz, 2H), 4.02 (q, J = 6.8, 2H), 2.23 (s, 3H), 1.09 (t, J = 6.8 Hz, 3H). ¹³C NMR (100 MHz, DMSO-*d*₆) δ 175.6, 172.8, 162.1, 155.3, 150.9, 143.7, 137.4, 134.9, 128.4, 128.3, 127.3, 127.2, 126.8, 93.5, 90.0, 75.2, 44.5, 35.7, 32.4, 20.6, 14.0. HRMS: calcd for C₂₅H₂₅N₄O₃ [M + H]⁺, 429.1921; found 429.1929.

1-Ethyl-7-phenethyl-5-(*p*-tolyl)-5,7,8,9-tetrahydro-1*H*-pyrrolo[3',4':5,6]pyrido[2,3-*d*]pyrimidine-2,4,6(3*H*)-trione (10c).

The title compound was prepared using the general procedure for the synthesis of the lactam analogs using chloromethyl intermediate **9** (50 mg, 0.12 mmol) and phenethylamine (17 mg, 0.14 mmol), which yielded a yellow solid (14 mg, 25%); mp 252 – 253 °C dec; 93% purity determined by UPLC. ¹H NMR (400 MHz, DMSO-*d*₆) δ 10.37 (s, 1H), 8.76 (s, 1H), 7.22 – 7.15 (m, 3H), 7.12 (d, J = 7.8 Hz, 2H), 7.06 – 6.97 (m, 4H), 5.13 (AB_q, J = 16.5 Hz, 1H), 5.00 (AB_q, J = 16.5 Hz, 1H), 4.85 (s, 1H), 4.00 (q, J = 7.2 Hz, 2H), 3.51 – 3.40 (m, 2H), 2.77 – 2.68 (m, 2H), 2.23 (s, 3H), 1.08 (t, J = 6.8 Hz, 3H). ¹³C NMR (100 MHz, DMSO-*d*₆) δ 175.1, 172.8, 162.1, 155.3, 150.9, 143.7, 138.3, 134.8, 128.7, 128.3, 128.2, 127.1, 126.2, 93.4, 89.8, 75.0, 43.0, 35.6, 35.2, 32.3, 20.6, 14.0. HRMS: calcd for C₂₆H₂₇N₄O₃ [M + H]⁺, 443.2078; found 443.2068.

1-Ethyl-7-(3-phenylpropyl)-5-(*p*-tolyl)-5,7,8,9-tetrahydro-1*H*-pyrrolo[3',4':5,6]pyrido[2,3-*d*]pyrimidine-2,4,6(3*H*)-trione (10d).

The title compound was prepared using the general procedure for the synthesis of the lactam analogs using chloromethyl intermediate **9** (50 mg, 0.12 mmol) and 3-phenylpropylamine (19 mg, 0.14 mmol), which yielded a yellow solid (15 mg, 28%); mp 244 – 245 °C dec; 98% purity determined by qNMR. ¹H NMR (400 MHz, DMSO-*d*₆) δ 10.38 (s, 1H), 8.68 (t, J = 6.0 Hz, 1H), 7.25 (t, J = 7.4 Hz, 2H), 7.21 – 7.11 (m, 3H), 7.06 (d, J = 7.5 Hz, 2H), 7.01 (d, J = 7.8 Hz, 2H), 5.26 (AB_q, J = 16.4 Hz, 1H), 5.09 (AB_q, J = 16.5 Hz, 1H), 4.90 (s, 1H), 4.02 (q, J = 6.9 Hz, 2H), 3.23 (d, J = 8.0 Hz, 2H), 2.40 (t, J = 7.8 Hz, 2H), 2.19 (s, 3H), 1.72 (p, J_1 = 4Hz, J_2 = 12Hz, 2H), 1.09 (t, J = 6.9 Hz, 3H). ¹³C NMR (100 MHz, DMSO-*d*₆) δ 175.1, 172.8, 162.1, 155.4, 150.9, 143.7, 141.0, 134.8, 128.3, 128.23, 128.17, 127.1, 125.8, 93.5, 89.8, 75.1, 40.8, 35.7, 32.4, 31.8, 30.6, 20.6, 14.0.

1-Ethyl-7-(2-phenoxyethyl)-5-(*p*-tolyl)-5,7,8,9-tetrahydro-1*H*-pyrrolo[3',4':5,6]pyrido[2,3-*d*]pyrimidine-2,4,6(3*H*)-trione (10e).

The title compound was prepared using the general procedure for the synthesis of the lactam analogs using chloromethyl intermediate **9** (50 mg, 0.12 mmol) and 2-phenoxyethylamine (19 mg, 0.14 mmol), which yielded a yellow solid (15 mg, 27%); mp 248 – 249 °C dec; 90% purity determined by qNMR. ¹H NMR (400 MHz, DMSO-*d*₆) δ 10.40 (s, 1H), 8.91 (t, J = 4 Hz, 1H), 7.27 (t, J = 8.1 Hz, 2H), 7.13 (d, J = 7.7 Hz, 2H), 6.94 (d, J = 7.3 Hz, 3H), 6.86 (d, J = 8.1 Hz, 2H), 5.29 (AB_q, J = 16.5 Hz, 1H), 5.10 (AB_q, J = 16.5 Hz, 1H), 4.92 (s, 1H), 4.09 – 3.96 (m, 4H), 3.70 – 3.53 (m, 2H), 2.17 (s, 3H), 1.09 (t, J = 6.9 Hz, 3H). ¹³C NMR (100 MHz, DMSO-*d*₆) δ 175.5, 173.1, 162.1, 158.0, 155.3, 150.9, 143.6, 134.7, 129.4, 128.4, 127.0, 120.8, 114.5, 93.4, 89.9, 75.1, 65.7, 41.1, 35.7, 32.1, 20.5, 14.0.

1-Ethyl-7-(1-methylpiperidin-4-yl)-5-(*p*-tolyl)-5,7,8,9-tetrahydro-1*H*-pyrrolo[3',4':5,6]pyrido[2,3-*d*]pyrimidine-2,4,6(3*H*)-trione (10f).

The title compound was prepared using the general procedure for the synthesis of the lactam analogs using chloromethyl intermediate **9** (50 mg, 0.12 mmol) and 4-amino-1-methylpiperidine (16 mg, 0.14 mmol), which yielded a yellow solid (5.2 mg, 10%); mp 248 – 249 °C dec; 89% purity determined by qNMR. ¹H NMR (400 MHz, DMSO-*d*₆) δ 10.42 (s, 1H), 8.77 (s, 1H), 7.16 (d, *J* = 7.7 Hz, 2H), 7.01 (d, *J* = 7.8 Hz, 2H), 5.27 (AB_q, *J* = 16.6 Hz, 1H), 5.09 (AB_q, *J* = 16.5 Hz, 1H), 4.99 (s, 1H), 4.02 (q, *J* = 7.3 Hz, 2H), 3.66 – 3.48 (m, 1H), 2.94 – 2.71 (m, 2H), 2.27 (s, 3H), 2.21 (s, 3H), 1.93 – 1.78 (m, 1H), 1.74 – 1.52 (m, 3H), 1.34–1.19 (m, 2H), 1.10 (t, *J* = 6.9 Hz, 3H).

7-(1-Benzylpiperidin-4-yl)-1-ethyl-5-(*p*-tolyl)-5,7,8,9-tetrahydro-1*H*-pyrrolo[3',4':5,6]pyrido[2,3-*d*]pyrimidine-2,4,6(3*H*)-trione (10g).

The title compound was prepared using the general procedure for the synthesis of the lactam analogs using chloromethyl intermediate **9** (50 mg, 0.12 mmol) and 4-amino-1-benzylpiperidine (27 mg, 0.14 mmol), which yielded a yellow solid (6.8 mg, 11%); mp 231 – 232 °C dec; 93% purity determined by qNMR. ¹H NMR (400 MHz, DMSO-*d*₆) δ 10.41 (s, 1H), 8.60 (s, 1H), 7.35 – 7.30 (m, 2H), 7.30 – 7.22 (m, 3H), 7.15 (d, *J* = 8.1 Hz, 2H), 7.01 (d, *J* = 7.7 Hz, 2H), 5.26 (AB_q, *J* = 16.5 Hz, 1H), 5.08 (AB_q, *J* = 16.4 Hz, 1H), 4.99 (s, 1H), 4.02 (q, *J* = 6.6 Hz, 2H), 3.55 (s, 1H), 3.43 (s, 2H), 2.84 – 2.59 (m, 2H), 2.21 (s, 3H), 2.09 – 1.89 (m, 2H), 1.80 (s, 1H), 1.69 – 1.41 (m, 3H), 1.10 (t, *J* = 6.9 Hz, 3H).

7-(1-Benzoylpiperidin-4-yl)-1-ethyl-5-(*p*-tolyl)-5,7,8,9-tetrahydro-1*H*-pyrrolo[3',4':5,6]pyrido[2,3-*d*]pyrimidine-2,4,6(3*H*)-trione (10h).

The title compound was prepared using the general procedure for the synthesis of the lactam analogs using chloromethyl intermediate **9** (50 mg, 0.12 mmol) and (4-aminopiperidin-1-yl)(phenyl)methanone (29 mg, 0.14 mmol), which yielded a yellow solid (20 mg, 31%); mp 226 – 227 °C dec; 95% purity determined by qNMR. ¹H NMR (400 MHz, DMSO-*d*₆) δ 10.43 (s, 1H), 8.64 (s, 1H), 7.47 – 7.41 (m, 3H), 7.33 – 7.28 (m, 2H), 7.14 (d, *J* = 7.8 Hz, 2H), 6.98 (d, *J* = 7.8 Hz, 2H), 5.29 (AB_q, *J* = 16.5 Hz, 1H), 5.10 (AB_q, *J* = 16.5 Hz, 1H), 4.97 (s, 1H), 4.30 (brs, 1H), 4.06 – 3.94 (m, 2H), 3.88 (s, 1H), 3.62 – 3.40 (m, 1H), 3.04 – 2.83 (m, 2H), 2.20 (s, 3H), 2.07 – 1.81 (m, 1H), 1.79 – 1.56 (m, 1H), 1.41 (s, 2H), 1.09 (t, *J* = 6.9 Hz, 3H).

7-((1-Benzylpiperidin-4-yl)methyl)-1-ethyl-5-(*p*-tolyl)-5,7,8,9-tetrahydro-1*H*-pyrrolo[3',4':5,6]pyrido[2,3-*d*]pyrimidine-2,4,6(3*H*)-trione (10i).

The title compound was prepared using the general procedure for the synthesis of the lactam analogs using chloromethyl intermediate **9** (50 mg, 0.12 mmol) and (1-benzylpiperidin-4-yl)methanamine (29 mg, 0.14 mmol), which yielded a yellow solid (13 mg, 20%); mp 216 – 217 °C dec; 89% purity determined by qNMR. ¹H NMR (400 MHz, DMSO-*d*₆) δ 10.39 (s, 1H), 8.63 (s, 1H), 7.36 – 7.27 (m, 2H), 7.29 – 7.23 (m, 3H), 7.14 (d, *J* = 8.1 Hz, 2H), 6.99 (d, *J* = 7.8 Hz, 2H), 5.26 (AB_q, *J* = 16.4 Hz, 1H), 5.10 (AB_q, *J* = 16.5 Hz, 1H), 4.90 (s, 1H), 4.07 – 3.96 (m, 2H), 3.40 (s, 2H), 3.18 – 3.03 (m, 2H), 2.77 – 2.64 (m, 2H), 2.19 (s, 3H), 1.79 (t, *J* = 12 Hz, 2H), 1.37 (brs, 3H), 1.16 – 0.97 (m, 5H).

1-Ethyl-7-((1-(4-nitrobenzyl)piperidin-4-yl)methyl)-5-(*p*-tolyl)-5,7,8,9-tetrahydro-1*H*-pyrrolo[3',4':5,6]pyrido[2,3-*d*]pyrimidine-2,4,6(3*H*)-trione (10j).

The title compound was prepared using the general procedure for the synthesis of the lactam analogs using chloromethyl intermediate **9** (50 mg, 0.12 mmol) and (1-(4-nitrobenzyl)piperidin-4-yl)methanamine (35 mg, 0.14 mmol), which yielded a yellow solid (7.5 mg, 11%); mp 167 – 168 °C dec; 95% purity determined by qNMR. ¹H NMR (400 MHz, DMSO-*d*₆) δ 10.38 (s, 1H), 8.63 (t, *J* = 6.2 Hz, 1H), 8.18 (d, *J* = 8.4 Hz, 2H), 7.55 (d, *J* = 8.4 Hz, 2H), 7.13 (d, *J* = 7.9 Hz, 2H), 6.98 (d, *J* = 7.8 Hz, 2H), 5.25 (AB_q, *J* = 16.5 Hz, 1H), 5.09 (AB_q, *J* = 16.5 Hz, 1H), 4.89 (s, 1H), 4.01 (q, *J* = 6.9 Hz, 2H), 3.54 (s, 2H), 3.11 (q, *J* = 6.9 Hz, 2H), 2.69 (t, *J* = 7.8 Hz, 2H), 2.17 (s, 3H), 1.85 (t, *J* = 11.2 Hz, 2H), 1.45 – 1.33 (m, 3H), 1.14 – 0.99 (m, 5H).

1-Ethyl-7-(4-methylphenethyl)-5-(*p*-tolyl)-5,7,8,9-tetrahydro-1*H*-pyrrolo[3',4':5,6]pyrido[2,3-*d*]pyrimidine-2,4,6(3*H*)-trione (10k).

The title compound was prepared using the general procedure for the synthesis of the lactam analogs using chloromethyl intermediate **9** (50 mg, 0.12 mmol) and 2-(*p*-tolyl)ethylamine (19 mg, 0.14 mmol), which yielded a yellow solid (17 mg, 31%); mp 189 – 190 °C dec; 99% purity determined by qNMR. ¹H NMR (400 MHz, DMSO-*d*₆) δ 10.37 (s, 1H), 8.74 (t, *J* = 5.6 Hz, 1H), 7.12 (d, *J* = 7.8 Hz, 2H), 7.03 – 6.96 (m, 4H), 6.90 (d, *J* = 7.7 Hz, 2H), 5.17 (AB_q, *J* = 16.5 Hz, 1H), 5.01 (AB_q, *J* = 16.5 Hz, 1H), 4.86 (s, 1H), 4.01 (q, *J* = 6.9 Hz, 2H), 3.41 – 3.36 (m, 2H), 2.75 – 2.61 (m, 2H), 2.23 (s, 6H), 1.09 (t, *J* = 6.9 Hz, 3H).

7-(4-Chlorophenethyl)-1-ethyl-5-(*p*-tolyl)-5,7,8,9-tetrahydro-1*H*-pyrrolo[3',4':5,6]pyrido[2,3-*d*]pyrimidine-2,4,6(3*H*)-trione (10l).

The title compound was synthesized using the general procedure for the synthesis of lactam analogs using chloromethyl intermediate **9** (50 mg, 0.12 mmol) and 2-(4-chlorophenyl)ethylamine (22 mg, 0.14 mmol), which yielded a yellow solid (8.6 mg, 15%); mp 159 – 161 °C dec; 98% purity determined by qNMR. ¹H NMR (400 MHz, DMSO-*d*₆) δ 10.38 (s, 1H), 8.70 (brs, 1H), 7.20 (d, *J* = 8.0 Hz, 2H), 7.10 (d, *J* = 7.8 Hz, 2H), 7.04 – 6.98 (m, 4H), 5.16 (AB_q, *J* = 16.5 Hz, 1H), 5.01 (AB_q, *J* = 16.4 Hz, 1H), 4.84 (s, 1H), 4.00 (q, *J* = 6.9 Hz, 2H), 3.54 – 3.40 (m, 2H), 2.81 – 2.65 (m, 2H), 2.24 (s, 3H), 1.08 (t, *J* = 6.9 Hz, 3H). ¹³C NMR (100 MHz, DMSO-*d*₆) δ 175.1, 172.8, 162.0, 155.3, 150.9, 143.6, 137.3, 134.8, 130.8, 130.6, 128.3, 128.1, 127.1, 93.4, 89.9, 75.1, 42.7, 35.7, 34.2, 32.3, 20.6, 14.0.

1-Ethyl-7-(4-hydroxyphenethyl)-5-(*p*-tolyl)-5,7,8,9-tetrahydro-1*H*-pyrrolo[3',4':5,6]pyrido[2,3-*d*]pyrimidine-2,4,6(3*H*)-trione (6a).²³

The title compound was prepared using the general procedure for the synthesis of the lactam analogs using chloromethyl intermediate **9** (50 mg, 0.12 mmol) and tyramine (19 mg, 0.14 mmol), which yielded a yellow solid (12 mg, 22%); mp 261 – 262 °C dec; 92% purity determined by UPLC. ¹H NMR (400 MHz, DMSO-*d*₆) δ 10.37 (s, 1H), 9.16 (s, 1H), 8.73 (s, 1H), 7.12 (d, *J* = 7.9 Hz, 2H), 7.01 (d, *J* = 7.9 Hz, 2H), 6.79 (d, *J* = 8.2 Hz, 2H), 6.57 (d, *J* = 8.2 Hz, 2H), 5.15 (AB_q, *J* = 16.4 Hz, 1H), 5.01 (AB_q, *J* = 16.4 Hz, 1H), 4.86 (s, 1H), 4.00 (q, *J* = 6.8 Hz, 2H), 3.41 – 3.33 (m, 2H), 2.62 – 2.49 (m, 2H), 2.23 (s, 3H), 1.08 (t, *J* = 6.8 Hz, 3H). ¹³C NMR (100 MHz, DMSO-*d*₆) δ 175.0, 172.8, 162.0, 155.7, 155.4, 150.9, 143.7,

134.8, 129.6, 128.3, 127.1, 115.0, 93.4, 89.8, 75.0, 43.4, 38.9, 35.6, 34.4, 32.3, 20.6, 14.0.
HRMS: calcd for C₂₆H₂₇N₄O₄ [M + H]⁺, 459.2027; found 459.2038.

1-Ethyl-7-(4-methoxyphenethyl)-5-(*p*-tolyl)-5,7,8,9-tetrahydro-1*H*-pyrrolo[3',4':5,6]pyrido[2,3-*d*]pyrimidine-2,4,6(3*H*)-trione (6b).²³

The title compound was prepared using the general procedure for the synthesis of the lactam analogs using chloromethyl intermediate **9** (50 mg, 0.12 mmol) and 2-(4-methoxyphenyl)ethylamine (21 mg, 0.14 mmol), which yielded a yellow solid (12 mg, 22%); mp 222 – 223 °C dec; 96% purity determined by UPLC. ¹H NMR (400 MHz, DMSO-*d*₆) δ 10.37 (s, 1H), 8.74 (s, 1H), 7.12 (d, *J* = 7.9 Hz, 2H), 7.02 (d, *J* = 7.9 Hz, 2H), 6.92 (d, *J* = 8.4 Hz, 2H), 6.73 (d, *J* = 8.4 Hz, 2H), 5.17 (AB_q, *J* = 16.5 Hz, 1H), 5.01 (AB_q, *J* = 16.5 Hz, 1H), 4.85 (s, 1H), 4.00 (q, *J* = 6.7 Hz, 2H), 3.70 (s, 3H), 3.44 – 3.37 (m, 2H), 2.70 – 2.62 (m, 2H), 2.23 (s, 3H), 1.08 (t, *J* = 6.7 Hz, 3H). ¹³C NMR (100 MHz, DMSO-*d*₆) δ 175.0, 172.8, 162.0, 157.7, 155.3, 150.9, 143.7, 134.8, 130.1, 129.7, 128.3, 127.1, 113.6, 93.4, 89.8, 75.0, 54.9, 43.2, 35.6, 34.2, 32.3, 20.6, 14.0. HRMS: calcd for C₂₇H₂₉N₄O₄ [M + H]⁺, 473.2183; found 473.2180.

1-Ethyl-7-(3-methoxyphenethyl)-5-(*p*-tolyl)-5,7,8,9-tetrahydro-1*H*-pyrrolo[3',4':5,6]pyrido[2,3-*d*]pyrimidine-2,4,6(3*H*)-trione (10m).

The title compound was prepared using the general procedure for the synthesis of the lactam analogs using chloromethyl intermediate **9** (50 mg, 0.12 mmol) and 2-(3-methoxyphenyl)ethylamine (21 mg, 0.14 mmol), which yielded a yellow solid (15 mg, 26%); mp 214 – 215 °C dec; 92% purity determined by qNMR. ¹H NMR (400 MHz, DMSO-*d*₆) δ 10.38 (s, 1H), 8.77 (s, 1H), 7.11 (d, *J* = 7.6 Hz, 3H), 6.99 (d, *J* = 7.8 Hz, 2H), 6.78 – 6.70 (m, 2H), 6.58 (d, *J* = 7.5 Hz, 1H), 5.19 (AB_q, *J* = 16.5 Hz, 1H), 5.01 (AB_q, *J* = 16.4 Hz, 1H), 4.87 (s, 1H), 4.01 (q, *J* = 6.9 Hz, 2H), 3.69 (s, 3H), 3.52 – 3.38 (m, 2H), 2.73 (t, *J* = 7.3 Hz, 2H), 2.21 (s, 3H), 1.08 (t, *J* = 6.9 Hz, 3H). ¹³C NMR (100 MHz, DMSO-*d*₆) δ 175.1, 172.8, 162.0, 159.2, 155.4, 150.9, 143.6, 139.8, 134.8, 129.3, 128.4, 127.0, 120.9, 114.3, 111.7, 93.4, 89.8, 75.1, 54.8, 42.9, 35.7, 35.1, 32.2, 20.6, 14.0.

1-Ethyl-7-(2-methoxyphenethyl)-5-(*p*-tolyl)-5,7,8,9-tetrahydro-1*H*-pyrrolo[3',4':5,6]pyrido[2,3-*d*]pyrimidine-2,4,6(3*H*)-trione (10n).

The title compound was prepared using the general procedure for the synthesis of the lactam analogs using chloromethyl intermediate **9** (50 mg, 0.12 mmol) and 2-(2-methoxyphenyl)ethylamine (21 mg, 0.14 mmol), which yielded a yellow solid (20 mg, 36%); mp 254 – 255 °C dec; 93% purity determined by qNMR. ¹H NMR (400 MHz, DMSO-*d*₆) δ 10.37 (s, 1H), 8.77 (s, 1H), 7.18 (t, *J* = 7.9 Hz, 1H), 7.12 (d, *J* = 7.8 Hz, 2H), 7.00 (d, *J* = 7.8 Hz, 2H), 6.92 (d, *J* = 8.2 Hz, 1H), 6.85 (d, *J* = 7.3 Hz, 1H), 6.74 (t, *J* = 7.4 Hz, 1H), 5.14 (AB_q, *J* = 16.5 Hz, 1H), 4.98 (AB_q, *J* = 16.5 Hz, 1H), 4.84 (s, 1H), 4.00 (q, *J* = 6.9 Hz, 2H), 3.74 (s, 3H), 3.41 (q, *J* = 6.7 Hz, 2H), 2.79 – 2.66 (m, 2H), 2.22 (s, 3H), 1.08 (t, *J* = 6.9 Hz, 3H). ¹³C NMR (100 MHz, DMSO-*d*₆) δ 175.0, 172.9, 162.0, 157.1, 155.4, 150.9, 143.7, 134.8, 130.2, 128.3, 127.8, 127.1, 125.9, 120.2, 110.5, 93.4, 89.8, 75.0, 55.2, 41.4, 35.6, 32.3, 30.2, 20.6, 14.0.

7-(3,4-Dimethoxyphenethyl)-1-ethyl-5-(*p*-tolyl)-5,7,8,9-tetrahydro-1*H*-pyrrolo[3',4':5,6]pyrido[2,3-*d*]pyrimidine-2,4,6(3*H*)-trione (10o).

The title compound was prepared using the general procedure for the synthesis of the lactam analogs using chloromethyl intermediate **9** (50 mg, 0.12 mmol) and 3,4-dimethoxyphenethylamine (25 mg, 0.14 mmol), which yielded a yellow solid (10 mg, 16%); mp 161 – 162 °C dec; 96% purity determined by qNMR. ¹H NMR (400 MHz, DMSO-*d*₆) δ 10.38 (s, 1H), 8.75 (s, 1H), 7.11 (d, *J* = 7.8 Hz, 2H), 6.99 (d, *J* = 7.8 Hz, 2H), 6.77 – 6.70 (m, 2H), 6.53 (d, *J* = 8.1 Hz, 1H), 5.22 (AB_q, *J* = 16.5 Hz, 1H), 5.02 (AB_q, *J* = 16.5 Hz, 1H), 4.88 (s, 1H), 4.01 (q, *J* = 6.7 Hz, 2H), 3.70 (s, 3H), 3.68 (s, 3H), 3.44 (q, *J* = 6.7 Hz, 2H), 2.69 (t, *J* = 7.1 Hz, 2H), 2.21 (s, 3H), 1.09 (t, *J* = 6.9 Hz, 3H). ¹³C NMR (100 MHz, DMSO-*d*₆) δ 175.1, 172.8, 162.0, 155.4, 150.9, 148.5, 147.3, 143.7, 134.8, 130.7, 128.3, 127.0, 120.6, 112.5, 111.7, 93.4, 89.8, 75.1, 55.4, 55.3, 43.1, 35.6, 34.6, 32.2, 20.6, 14.0.

7-(2,3-Dimethoxyphenethyl)-1-ethyl-5-(*p*-tolyl)-5,7,8,9-tetrahydro-1*H*-pyrrolo[3',4':5,6]pyrido[2,3-*d*]pyrimidine-2,4,6(3*H*)-trione (10p).

The title compound was prepared using the general procedure for the synthesis of the lactam analogs using chloromethyl intermediate **9** (50 mg, 0.12 mmol) and 2,3-dimethoxyphenethylamine (25 mg, 0.14 mmol), which yielded a yellow solid (11 mg, 18%); mp 255 – 256 °C dec; 97% purity determined by qNMR. ¹H NMR (400 MHz, DMSO-*d*₆) δ 10.37 (s, 1H), 8.79 (s, 1H), 7.11 (d, *J* = 7.8 Hz, 2H), 7.00 (d, *J* = 7.8 Hz, 2H), 6.87 (q, *J* = 8.4 Hz, 2H), 6.50 (d, *J* = 7.0 Hz, 1H), 5.18 (AB_q, *J* = 16.5 Hz, 1H), 5.02 (AB_q, *J* = 16.4 Hz, 1H), 4.84 (s, 1H), 4.01 (q, *J* = 6.9 Hz, 2H), 3.77 (s, 3H), 3.67 (s, 3H), 3.46 – 3.36 (m, 2H), 2.79 – 2.64 (m, 2H), 2.22 (s, 3H), 1.09 (t, *J* = 6.9 Hz, 3H).

7-(3,4-Dichlorophenethyl)-1-ethyl-5-(*p*-tolyl)-5,7,8,9-tetrahydro-1*H*-pyrrolo[3',4':5,6]pyrido[2,3-*d*]pyrimidine-2,4,6(3*H*)-trione (10q).

The title compound was prepared using the general procedure for the synthesis of the lactam analogs using chloromethyl intermediate **9** (50 mg, 0.12 mmol) and 3,4-dichlorophenethylamine (27 mg, 0.14 mmol), which yielded a yellow solid (7.9 mg, 13%); 97% purity determined by qNMR. ¹H NMR (400 MHz, DMSO-*d*₆) δ 10.39 (s, 1H), 8.69 (s, 1H), 7.44 (s, 1H), 7.37 (d, *J* = 8.2 Hz, 1H), 7.08 (d, *J* = 7.8 Hz, 2H), 7.01 – 6.92 (m, 3H), 5.19 (AB_q, *J* = 16.5 Hz, 1H), 5.02 (AB_q, *J* = 16.5 Hz, 1H), 4.85 (s, 1H), 4.00 (q, *J* = 6.9 Hz, 2H), 3.56 – 3.39 (m, 2H), 2.87 – 2.69 (m, 2H), 2.22 (s, 3H), 1.08 (t, *J* = 6.9 Hz, 3H). ¹³C NMR (100 MHz, DMSO-*d*₆) δ 175.2, 172.8, 162.0, 155.3, 150.9, 143.5, 139.6, 134.8, 130.8, 130.7, 130.2, 129.2, 128.9, 128.3, 127.0, 93.3, 89.8, 75.1, 42.3, 35.7, 33.8, 32.2, 20.6, 14.0.

Ethyl 2-(4-(2-(1-Ethyl-2,4,6-trioxo-5-(*p*-tolyl)-1,2,3,4,5,6,8,9-octahydro-7*H*-pyrrolo[3',4':5,6]pyrido[2,3-*d*]pyrimidin-7-yl)ethyl)phenoxy)acetate (ethyl ester of 10r).

The title compound was prepared using the general procedure for the synthesis of the lactam analogs using chloromethyl intermediate **9** (50 mg, 0.12 mmol) and ethyl 2-(4-(2-aminoethyl)phenoxy)acetate (31 mg, 0.14 mmol), which yielded a yellow solid (25 mg, 37%) that was directly subjected to hydrolysis. ¹H NMR (400 MHz, DMSO-*d*₆) δ 10.38 (s, 1H), 8.75 (s, 1H), 7.14 (d, *J* = 7.8 Hz, 2H), 7.04 (d, *J* = 7.8 Hz, 2H), 6.90 (d, *J* = 8.1 Hz, 2H), 6.72 (d, *J* = 8.2 Hz, 2H), 5.12 (AB_q, *J* = 16.5 Hz, 1H), 5.00 (AB_q, *J* = 16.5 Hz, 1H), 4.86 (s,

1H), 4.73 (s, 2H), 4.17 (q, $J = 7.1$ Hz, 2H), 4.02 (q, $J = 7.1$ Hz, 2H), 3.49 – 3.37 (m, 2H), 2.74 – 2.63 (m, 2H), 2.25 (s, 3H), 1.22 (t, $J = 7.1$ Hz, 3H), 1.10 (t, $J = 6.9$ Hz, 3H).

Methyl 4-((4-((1-Ethyl-2,4,6-trioxo-5-(*p*-tolyl)-1,2,3,4,5,6,8,9-octahydro-7H-pyrrolo[3',4':5,6]pyrido[2,3-*d*]pyrimidin-7-yl)methyl)piperidin-1-yl)methyl)benzoate (methyl ester of 10s).

The title compound was prepared using the general procedure for the synthesis of lactam analogs using chloromethyl intermediate **9** (100 mg, 0.24 mmol) and methyl 4-((4-(aminomethyl)piperidin-1-yl)methyl)benzoate (73 mg, 0.28 mmol), which yielded a yellow solid (57 mg, 41%). ¹H NMR (400 MHz, DMSO-*d*₆) δ 10.39 (s, 1H), 8.64 (s, 1H), 7.92 (d, $J = 7.9$ Hz, 2H), 7.43 (d, $J = 8.0$ Hz, 2H), 7.14 (d, $J = 7.7$ Hz, 2H), 6.99 (d, $J = 7.7$ Hz, 2H), 5.32 – 5.18 (m, 1H), 5.19 – 5.01 (m, 1H), 4.90 (s, 1H), 4.02 (d, $J = 7.7$ Hz, 2H), 3.85 (s, 3H), 3.49 (s, 2H), 3.11 (brs, 2H), 2.72 (sbr, 2H), 2.18 (s, 3H), 1.83 (t, $J = 11.5$ Hz, 2H), 1.39 (brs, 3H), 1.10 (brt, $J = 6.9$ Hz, 5H).

Methyl 4-(2-(1-Ethyl-2,4,6-trioxo-5-(*p*-tolyl)-1,2,3,4,5,6,8,9-octahydro-7H-pyrrolo[3',4':5,6]pyrido[2,3-*d*]pyrimidin-7-yl)ethyl)benzoate (methyl ester of 10t).

The title compound was prepared using the general procedure for the synthesis of the lactam analogs using chloromethyl intermediate **9** (50 mg, 0.12 mmol) and methyl 4-(2-aminoethyl)benzoate (25 mg, 0.14 mmol), which yielded a yellow solid (42 mg, 69%). ¹H NMR (400 MHz, DMSO-*d*₆) δ 10.39 (s, 1H), 8.74 (s, 1H), 7.76 (d, $J = 7.9$ Hz, 2H), 7.12 (dd, $J = 11.0, 7.9$ Hz, 4H), 7.01 (d, $J = 7.8$ Hz, 2H), 5.17 (AB_q, $J = 16.5$ Hz, 1H), 5.02 (AB_q, $J = 16.5$ Hz, 1H), 4.85 (s, 1H), 4.01 (q, $J = 6.8$ Hz, 2H), 3.85 (s, 3H), 3.58 – 3.51 (m, 1H), 3.51 – 3.44 (m, 1H), 3.62 – 3.39 (m, 2H), 2.92 – 2.75 (m, 2H), 2.26 (s, 3H), 1.10 (t, $J = 6.9$ Hz, 3H).

Methyl 4-((1-Ethyl-2,4,6-trioxo-5-(*p*-tolyl)-1,2,3,4,5,6,8,9-octahydro-7H-pyrrolo[3',4':5,6]pyrido[2,3-*d*]pyrimidin-7-yl)methyl)benzoate (methyl ester of 10u).

The title compound was prepared using the general procedure for the synthesis of the lactam analogs using chloromethyl intermediate **9** (100 mg, 0.24 mmol) and methyl 4-(aminomethyl)benzoate (46 mg, 0.28 mmol), which yielded a yellow solid (41 mg, 42%). ¹H NMR (400 MHz, DMSO-*d*₆) δ 10.44 (s, 1H), 9.21 (s, 1H), 7.87 (d, $J = 8.0$ Hz, 2H), 7.20 (t, $J = 8.0$ Hz, 4H), 7.05 (d, $J = 7.7$ Hz, 2H), 5.29 (AB_q, $J = 16.6$ Hz, 1H), 5.13 (AB_q, $J = 16.6$ Hz, 1H), 4.93 (s, 1H), 4.55 (d, $J = 5.9$ Hz, 2H), 4.03 (q, $J = 6.8$ Hz, 2H), 3.85 (s, 3H), 2.25 (s, 3H), 1.11 (t, $J = 6.9$ Hz, 3H).

Methyl 3-((1-Ethyl-2,4,6-trioxo-5-(*p*-tolyl)-1,2,3,4,5,6,8,9-octahydro-7H-pyrrolo[3',4':5,6]pyrido[2,3-*d*]pyrimidin-7-yl)methyl)benzoate (methyl ester of 10v).

The title compound was prepared using the general procedure for the synthesis of the lactam analogs using chloromethyl intermediate **9** (100 mg, 0.24 mmol) and methyl 3-(aminomethyl)benzoate (46 mg, 0.28 mmol), which yielded a yellow solid (44 mg, 45%). ¹H NMR (400 MHz, DMSO-*d*₆) δ 10.44 (s, 1H), 9.25 (s, 1H), 7.86 (d, $J = 8.1$ Hz, 2H), 7.45 (t, $J = 7.7$ Hz, 1H), 7.37 (d, $J = 7.7$ Hz, 1H), 7.17 (d, $J = 7.7$ Hz, 2H), 7.02 (d, $J = 7.6$ Hz, 2H),

5.30 (AB_q, *J* = 16.6 Hz, 1H), 5.12 (AB_q, *J* = 16.7 Hz, 1H), 4.93 (s, 1H), 4.54 (brs, 2H), 4.03 (d, *J* = 7.3 Hz, 2H), 3.87 (s, 3H), 2.23 (s, 3H), 1.10 (t, *J* = 6.9 Hz, 3H).

General Procedure for the Synthesis of the Dihydropyridine Lactam Derivatives with Free Carboxylate Groups:

The methyl or ethyl ester precursor (1 equiv) was dissolved in methanol/water (1:1). After the addition of lithium hydroxide monohydrate (7 equiv), the mixture was stirred at room temperature overnight. Upon the consumption of the starting material monitored by TLC, the mixture was extracted with EtOAc and the aqueous layer was kept and acidified with a 1 M HCl solution. The precipitated solid was collected via filtration and dried under reduced pressure to yield the target molecule.

2-(4-(2-(1-Ethyl-2,4,6-trioxo-5-(*p*-tolyl)-1,2,3,4,5,6,8,9-octahydro-7H-pyrrolo[3',4':5,6]pyrido[2,3-*d*]pyrimidin-7-yl)ethyl)phenoxy)acetic Acid (10r).

The title compound was synthesized via the general procedure of lactam analog with free carboxylate groups using ethyl 2-(4-(2-(1-ethyl-2,4,6-trioxo-5-(*p*-tolyl)-1,2,3,4,5,6,8,9-octahydro-7H-pyrrolo[3',4':5,6]pyrido[2,3-*d*]pyrimidin-7-yl)ethyl)phenoxy)acetate (25 mg, 0.044 mmol), which yielded a yellow solid (10 mg, 43%); mp 281 – 282 °C dec, 98% purity determined by qNMR. ¹H NMR (400 MHz, DMSO-*d*₆) δ 13.02 (br, 1H), 10.38 (s, 1H), 8.77 (s, 1H), 7.14 (d, *J* = 7.8 Hz, 2H), 7.04 (d, *J* = 7.8 Hz, 2H), 6.90 (d, *J* = 8.1 Hz, 2H), 6.71 (d, *J* = 8.1 Hz, 2H), 5.17 (AB_q, *J* = 16.5 Hz, 1H), 5.02 (AB_q, *J* = 16.5 Hz, 1H), 4.87 (s, 1H), 4.60 (s, 2H), 4.02 (q, *J* = 7.0, 6.6 Hz, 2H), 3.50 – 3.33 (m, 2H), 2.74 – 2.58 (m, 2H), 2.25 (s, 3H), 1.10 (t, *J* = 6.9 Hz, 3H).

4-((4-((1-Ethyl-2,4,6-trioxo-5-(*p*-tolyl)-1,2,3,4,5,6,8,9-octahydro-7H-pyrrolo[3',4':5,6]pyrido[2,3-*d*]pyrimidin-7-yl)methyl)piperidin-1-yl)methyl)benzoate (10s).

The title compound was synthesized via the general procedure of lactam analogs with free carboxylate groups using methyl 4-((4-((1-ethyl-2,4,6-trioxo-5-(*p*-tolyl)-1,2,3,4,5,6,8,9-octahydro-7H-pyrrolo[3',4':5,6]pyrido[2,3-*d*]pyrimidin-7-yl)methyl)piperidin-1-yl)methyl)benzoate (57 mg, 0.098 mmol), which yielded a yellow solid (25 mg, 45%); mp 305 – 306 °C dec. 90% purity determined by UPLC. ¹H NMR (400 MHz, DMSO-*d*₆) δ 13.21 (br, 1H), 10.39 (s, 1H), 8.69 (s, 1H), 7.87 (d, *J* = 7.8 Hz, 2H), 7.33 (d, *J* = 7.8 Hz, 2H), 7.15 (d, *J* = 7.7 Hz, 2H), 6.99 (d, *J* = 7.7 Hz, 2H), 5.25 (AB_q, *J* = 16.5 Hz, 1H), 5.10 (AB_q, *J* = 16.4 Hz, 1H), 4.91 (s, 1H), 4.02 (q, *J* = 6.9 Hz, 2H), 3.46 (s, 2H), 3.20 – 3.04 (m, 2H), 2.71 (d, *J* = 11.3 Hz, 2H), 2.19 (s, 3H), 1.81 (t, *J* = 11.3 Hz, 2H), 1.45 – 1.30 (m, 3H), 1.10 (m, 5H).

4-(2-(1-Ethyl-2,4,6-trioxo-5-(*p*-tolyl)-1,2,3,4,5,6,8,9-octahydro-7H-pyrrolo[3',4':5,6]pyrido[2,3-*d*]pyrimidin-7-yl)ethyl)benzoic Acid (10t).

The title compound was synthesized via the general procedure of lactam analog with free carboxylate groups using methyl 4-(2-(1-ethyl-2,4,6-trioxo-5-(*p*-tolyl)-1,2,3,4,5,6,8,9-octahydro-7H-pyrrolo[3',4':5,6]pyrido[2,3-*d*]pyrimidin-7-yl)ethyl)benzoate (42 mg, 0.084 mmol), which yielded a yellow solid (12 mg, 29%); mp 316 – 317 °C dec; 98% purity

determined by qNMR. ¹H NMR (400 MHz, DMSO-*d*₆) δ 12.83 (s, 1H), 10.39 (s, 1H), 8.75 (s, 1H), 7.75 (d, *J* = 7.8 Hz, 2H), 7.11 (d, *J* = 7.8 Hz, 4H), 7.01 (d, *J* = 7.8 Hz, 2H), 5.17 (AB_q, *J* = 16.5 Hz, 1H), 5.02 (AB_q, *J* = 16.5 Hz, 1H), 4.85 (s, 1H), 4.01 (q, *J* = 6.9 Hz, 2H), 3.64 – 3.40 (m, 2H), 2.91 – 2.74 (m, 2H), 2.25 (s, 3H), 1.09 (t, *J* = 6.9 Hz, 3H).

4-((1-Ethyl-2,4,6-trioxo-5-(*p*-tolyl)-1,2,3,4,5,6,8,9-octahydro-7*H*-pyrrolo[3',4':5,6]pyrido[2,3-*d*]pyrimidin-7-yl)methyl)benzoic Acid (10u).

Title compound was synthesized via the general procedure of lactam analog with free carboxylate groups using methyl 4-((1-ethyl-2,4,6-trioxo-5-(*p*-tolyl)-1,2,3,4,5,6,8,9-octahydro-7*H*-pyrrolo[3',4':5,6]pyrido[2,3-*d*]pyrimidin-7-yl)methyl)benzoate (41 mg, 0.084 mmol), which yielded a yellow solid (15 mg, 39%); mp 345 – 346 °C dec, 95% purity determined by qNMR. ¹H NMR (400 MHz, DMSO-*d*₆) δ 12.92 (s, 1H), 10.44 (s, 1H), 9.21 (s, 1H), 7.84 (d, *J* = 8.0 Hz, 2H), 7.18 (dd, *J* = 7.9, 5.4 Hz, 4H), 7.04 (d, *J* = 7.7 Hz, 2H), 5.29 (AB_q, *J* = 16.7 Hz, 1H), 5.13 (AB_q, *J* = 16.6 Hz, 1H), 4.93 (s, 1H), 4.58 – 4.48 (m, 2H), 4.03 (q, *J* = 7.2 Hz, 2H), 2.25 (s, 3H), 1.10 (t, *J* = 6.9 Hz, 3H).

3-((1-Ethyl-2,4,6-trioxo-5-(*p*-tolyl)-1,2,3,4,5,6,8,9-octahydro-7*H*-pyrrolo[3',4':5,6]pyrido[2,3-*d*]pyrimidin-7-yl)methyl)benzoic Acid (10v).

Title compound was synthesized via the general procedure of lactam analog with free carboxylate groups using methyl 4-((1-ethyl-2,4,6-trioxo-5-(*p*-tolyl)-1,2,3,4,5,6,8,9-octahydro-7*H*-pyrrolo[3',4':5,6]pyrido[2,3-*d*]pyrimidin-7-yl)methyl)benzoate (44 mg, 0.090 mmol), which yielded a yellow solid (7.7 mg, 18%); mp 269 – 270 °C dec, 98% purity determined by qNMR. ¹H NMR (400 MHz, DMSO-*d*₆) δ 13.02 (s, 1H), 10.43 (s, 1H), 9.24 (s, 1H), 7.84 (d, *J* = 6.8 Hz, 2H), 7.42 (t, *J* = 7.8 Hz, 1H), 7.33 (d, *J* = 7.8 Hz, 1H), 7.17 (d, *J* = 7.7 Hz, 2H), 7.02 (d, *J* = 7.6 Hz, 2H), 5.30 (AB_q, *J* = 16.6 Hz, 1H), 5.12 (AB_q, *J* = 16.6 Hz, 1H), 4.93 (s, 1H), 4.54 (d, *J* = 5.7 Hz, 2H), 4.03 (q, *J* = 6.8 Hz, 2H), 2.23 (s, 3H), 1.10 (t, *J* = 6.9 Hz, 3H).

BRD4-1, BRD4-2, BRDT-1 and BRDT-2 AlphaScreen Assays.

The assays were performed with minor modifications from the manufacturer's protocol (Perkin Elmer, USA). All reagents were diluted in AlphaScreen™ buffer (50 mM HEPES, 150 mM NaCl, 0.01% v/v Tween-20, 0.1% w/v BSA, pH 7.4). After addition of the Alpha beads to the master solutions, all subsequent steps were performed under low light conditions. A 2x solution of components with final concentrations of His-BRD4-1, His-BRD4-2, His-BRDT-1, His-BRDT-2 at 20 nM, Ni-coated acceptor bead at 10 µg/ml, and biotinylated-JQ1 at 10 nM was added in 10 µL to 384-well plates (AlphaPlate-384, PerkinElmer). Plates were spun down at 1000 rpm. A 10-point 1:√¹⁰ serial dilution of compounds in DMSO was prepared at 200 × the final concentration. Compound (100 nL) from these stock plates was added by pin transfer using a Janus Workstation (PerkinElmer). A 2x solution of streptavidin-coated donor beads with a final concentration of 10 µg/mL was added in a 10 µL volume. The plates were spun down again at 1000 rpm and sealed with foil to prevent light exposure and evaporation. The plates were then incubated at room temperature for 1 hour and read on an Envision 2104 (PerkinElmer) using the manufacturer's protocol. IC₅₀ values were calculated using a 4-parameter logistic curve

in Prism 6 (GraphPad Software, USA) after normalization to DMSO-treated negative control wells.

Protein Crystallography.

BRD4-1 was purified as described.⁴⁴ Crystals were grown by vapor-diffusion in hanging drops using 0.2 M NaCl, 0.1 M HEPES pH 7.5, 25% (w/v) polyethylene glycol 3,350 as precipitant supplemented with 1 mM compound **10j** and 10% (v/v) DMSO. Crystals were harvested in cryoprotectant (precipitant + 25% (v/v) ethylene glycol) and flash frozen in a stream of nitrogen gas. X-ray diffraction data were recorded at beamline 22-BM (SER-CAT) of the Advanced Photon Source. Data were reduced and scaled with XDS.⁴⁵ PHENIX⁴⁶ was employed for phasing and refinement, and model building was performed using Coot.⁴⁷ The structure was solved by molecular replacement using PDB entry 5VBP as search model. An initial model of the inhibitor was generated with ligand restraints from eLBOW of the PHENIX suite. All structures were validated by MolProbity⁴⁸ and phenix.model_vs_data.⁴⁹ 2D interaction diagrams were computed with Poseview.⁵⁰ Data collection and refinement statistics are shown in Supplementary Table S1. Atomic coordinates and structure factors have been deposited in the Protein Data Bank (PDB) under accession code 7LH8.

Fluorinated Protein Expression and Purification.

The 5-fluorotryptophan-labeled BRDT-T protein residues (2–416) was expressed as previously described.⁴⁰ To the cell pellet containing overexpressed BRDT-T was added 40 mL of lysis buffer (50 mM phosphate, 300 mM NaCl, pH 7.4) and 40 mg phenylmethanesulfonyl fluoride (PMSF), and the mixture was allowed to thaw at room temperature for 30 min. Cells were put on ice and sonicated in 30-second intervals followed by 60 seconds of cooling for a total of 12 min of sonication time. The lysed cells were centrifuged at 10000 *xg* for 30 min. The supernatant was decanted from the pelleted cell debris and filtered using Whatman filter paper. Ni affinity purification was done using a Ni HisTrap FF 5 mL column (GE Healthcare) on an AKTA Fast Protein Liquid Chromatography (FPLC) system by monitoring the absorbance at 280 nm. BRDT-T was eluted with a 0–100% gradient of wash buffer (50 mM phosphate, 100 mM NaCl, 40 mM imidazole, pH 7.4) and elution buffer (50 mM phosphate, 100 mM NaCl, 400 mM imidazole, pH 7.4) across 20 column volumes. Purified protein was then buffer exchanged into storage buffer (50 mM HEPES, 100 mM NaCl, pH 7.4) using a HiPrep desalting column (GE Healthcare) equilibrated with 1 column volume of buffer. Protein purity was assessed using SDS-polyacrylamide gel electrophoresis (12% Bis-Tris, 1.0 mM gels. Running conditions: 120 V, 90 min in MES buffer). Protein was concentrated to ~25–35 μ M using Amicon Ultra-15 (Millipore) centrifugal filters with either a 3 kDa or a 10 kDa molecular weight cut off (MWCO = 3000 Da or 10000 Da), flash frozen and stored at –20 °C. Quadrupole Time-of-Flight (Q-TOF) LC/MS was used to confirm the identity of the protein and determine percent fluorine incorporation using the following equation.

$$\% \text{ Incorporation} = \frac{(0 F \text{ protein}^*0) + (1F \text{ protein}^*1) + \dots (nF \text{ protein}^*n)}{(0F \text{ protein}^*n) + (1F \text{ protein}^*n) + \dots (nF \text{ protein}^*n)} * 100$$

Protein masses and fluorine incorporation are shown in Table S2.

Protein-Observed Fluorine NMR (PrOF NMR).

Experiments were run on a Bruker 600-MHz Avance NEO (6002), equipped with a 5-mm triple resonance cryoprobe. 5FW-labeled BRDT-T was diluted in 50 mM HEPES, 100 mM NaCl, pH = 7.4 buffer by the addition of D₂O and 0.1% TFA to final concentrations of 4% and 0.4% respectively. Two one-dimensional ¹⁹F NMR spectra were taken of the control protein sample at an O1P of -75 ppm, NS = 16, D1 = 1 s, AQ = 0.5 s (TFA reference set to -75.25 ppm) and an O1P of -125 ppm, NS = 3072, D1 = 0.6 s, AQ = 0.05 s (protein resonances). Ligand stock solutions of 10–50 mM prepared in DMSO were titrated into the bromodomain protein solution (27 μM). The change in chemical shift of the protein resonance ($\Delta\delta_{obs}$) was plotted as a function of ligand concentration to generate binding isotherms using Equation 1: $\Delta\delta_{max}$ is the maximum change in fluorine chemical shift, [L] is the concentration of ligand, and [P] is the concentration of protein, and [PL] is the concentration of bound complex.

$$\Delta\delta_{obs} = \Delta\delta_{max} \times \frac{(K_d + [L] + [P]) - \sqrt{(K_d + [L] + [P])^2 - 4[PL]}}{2[PL]} \quad \text{Eq. 1}$$

Supplementary Material

Refer to Web version on PubMed Central for supplementary material.

Acknowledgements

This project was supported by the NIH/NICHD: HHSN275201300017C and 5P50HD093540 from the Contraception Research Branch. We thank the Moffitt Chemical Biology Core for use of the protein crystallography facility (NCI grant 5P30-CA076292).

References

1. Choudhary C; Kumar C; Gnad F; Nielsen ML; Rehman M; Walther TC; Olsen JV; Mann M Lysine acetylation targets protein complexes and co-regulates major cellular functions. *Science* 2009, 325, 834–840. [PubMed: 19608861]
2. Zhao S; Xu W; Jiang W; Yu W; Lin Y; Zhang T; Yao J; Zhou L; Zeng Y; Li H; Li Y; Shi J; An W; Hancock SM; He F; Qin L; Chin J; Yang P; Chen X; Lei Q; Xiong Y; Guan KL Regulation of cellular metabolism by protein lysine acetylation. *Science* 2010, 327, 1000–1004. [PubMed: 20167786]
3. Filippakopoulos P; Picaud S; Mangos M; Keates T; Lambert JP; Barsyte-Lovejoy D; Felletar I; Volkmer R; Muller S; Pawson T; Gingras AC; Arrowsmith CH; Knapp S Histone recognition and large-scale structural analysis of the human bromodomain family. *Cell* 2012, 149, 214–231. [PubMed: 22464331]
4. Verdin E; Ott M 50 years of protein acetylation: from gene regulation to epigenetics, metabolism and beyond. *Nat. Rev. Mol. Cell Biol* 2015, 16, 258–264. [PubMed: 25549891]
5. Kouzarides T Acetylation: a regulatory modification to rival phosphorylation? *EMBO J.* 2000, 19, 1176–1179. [PubMed: 10716917]

6. Devaiah BN; Case-Borden C; Gegonne A; Hsu CH; Chen Q; Meerzaman D; Dey A; Ozato K; Singer DS BRD4 is a histone acetyltransferase that evicts nucleosomes from chromatin. *Nat. Struct. Mol. Biol* 2016, 23, 540–548. [PubMed: 27159561]
7. Fenley AT; Anandakrishnan R; Kidane YH; Onufriev AV Modulation of nucleosomal DNA accessibility via charge-altering post-translational modifications in histone core. *Epigenetics Chromatin* 2018, 11, 11. [PubMed: 29548294]
8. Bechter O; Schöffski P Make your best BET: The emerging role of BET inhibitor treatment in malignant tumors. *Pharmacol. Ther* 2020, 208, 107479. [PubMed: 31931101]
9. Zeng L; Zhou MM Bromodomain: an acetyl-lysine binding domain. 2002, 513, 124–128.
10. Alekseyenko AA; Walsh EM; Zee BM; Pakozdi T; Hsi P; Lemieux ME; Dal Cin P; Ince TA; Kharchenko PV; Kuroda MI; French CA Ectopic protein interactions within BRD4-chromatin complexes drive oncogenic megadomain formation in NUT midline carcinoma. *Proc. Natl. Acad. Sci. U. S. A* 2017, 114, E4184–E4192. [PubMed: 28484033]
11. Shang E; Salazar G; Crowley TE; Wang X; Lopez RA; Wang X; Wolgemuth DJ Identification of unique, differentiation stage-specific patterns of expression of the bromodomain-containing genes Brd2, Brd3, Brd4, and Brdt in the mouse testis. *Gene Expr. Patterns* 2004, 4, 513–519. [PubMed: 15261828]
12. Brown JD; Feldman ZB; Doherty SP; Reyes JM; Rahl PB; Lin CY; Sheng Q; Duan Q; Federation AJ; Kung AL; Haldar SM; Young RA; Plutzky J; Bradner JE BET bromodomain proteins regulate enhancer function during adipogenesis. *Proc. Natl. Acad. Sci. U. S. A* 2018, 115, 2144–2149. [PubMed: 29444854]
13. Shang E; Nickerson HD; Wen D; Wang X; Wolgemuth DJ The first bromodomain of Brdt, a testis-specific member of the BET sub-family of double-bromodomain-containing proteins, is essential for male germ cell differentiation. *Development* 2007, 134, 3507–3515. [PubMed: 17728347]
14. Berkovits BD; Wolgemuth DJ The first bromodomain of the testis-specific double bromodomain protein Brdt is required for chromocenter organization that is modulated by genetic background. *Dev. Biol* 2011, 360, 358–368. [PubMed: 22020252]
15. Barda S; Paz G; Yogev L; Yavetz H; Lehavi O; Hauser R; Botchan A; Breitbart H; Kleiman SE Expression of BET genes in testis of men with different spermatogenic impairments. *Fertil. Steril* 2012, 97, 46–52 e45. [PubMed: 22035730]
16. Gaucher J; Boussouar F; Montellier E; Curtet S; Buchou T; Bertrand S; Hery P; Jounier S; Depaux A; Vitte A-L; Guardiola P; Pernet K; Debernardi A; Lopez F; Holota H; Imbert J; Wolgemuth DJ; Gérard M; Rousseaux S; Khochbin S Bromodomain-dependent stage-specific male genome programming by Brdt. *EMBO J.* 2012, 31, 3809–3820. [PubMed: 22922464]
17. Matzuk MM; McKeown MR; Filippakopoulos P; Li Q; Ma L; Agno JE; Lemieux ME; Picaud S; Yu RN; Qi J; Knapp S; Bradner JE Small-molecule inhibition of BRDT for male contraception. *Cell* 2012, 150, 673–684. [PubMed: 22901802]
18. Yu Z; Ku AF; Anglin JL; Sharma R; Ucisik MN; Faver JC; Li F; Nyshadham P; Simmons N; Sharma KL; Nagarajan S; Riehle K; Kaur G; Sankaran B; Storl-Desmond M; Palmer SS; Young DW; Kim C; Matzuk MM Discovery and characterization of bromodomain 2-specific inhibitors of BRDT. *Proc. Natl. Acad. Sci. U. S. A* 2021, 118, e2021102118. [PubMed: 33637650]
19. Filippakopoulos P; Qi J; Picaud S; Shen Y; Smith WB; Fedorov O; Morse EM; Keates T; Hickman TT; Felletar I; Philpott M; Munro S; McKeown MR; Wang Y; Christie AL; West N; Cameron MJ; Schwartz B; Heightman TD; La Thangue N; French CA; Wiest O; Kung AL; Knapp S; Bradner JE Selective inhibition of BET bromodomains. *Nature* 2010, 468, 1067–1073. [PubMed: 20871596]
20. Mirguet O; Lamotte Y; Chung CW; Bamborough P; Delannee D; Bouillot A; Gellibert F; Krysa G; Lewis A; Witherington J; Huet P; Dudit Y; Trotter L; Nicodeme E Naphthyridines as novel BET family bromodomain inhibitors. *ChemMedChem* 2014, 9, 580–589. [PubMed: 24000170]
21. McDaniel KF; Wang L; Soltwedel T; Fidanze SD; Hasvold LA; Liu D; Mantei RA; Pratt JK; Sheppard GS; Bui MH; Faivre EJ; Huang X; Li L; Lin X; Wang R; Warder SE; Wilcox D; Albert DH; Magoc TJ; Rajaraman G; Park CH; Hutchins CW; Shen JJ; Edalji RP; Sun CC; Martin R; Gao W; Wong S; Fang G; Elmore SW; Shen Y; Kati WM Discovery of N-(4-(2,4-difluorophenoxy)-3-(6-methyl-7-oxo-6,7-dihydro-1H-pyrrolo[2,3-c]pyridin-4-yl)phenyl)ethanesulfonamide (ABBV-075/Mivebresib), a potent and orally available

- bromodomain and extraterminal domain (BET) family bromodomain inhibitor. *J. Med. Chem* 2017, 60, 8369–8384. [PubMed: 28949521]
22. Picaud S; Wells C; Felletar I; Brotherton D; Martin S; Savitsky P; Diez-Dacal B; Philpott M; Bountra C; Lingard H; Fedorov O; Muller S; Brennan PE; Knapp S; Filippakopoulos P RVX-208, an inhibitor of BET transcriptional regulators with selectivity for the second bromodomain. *Proc. Natl. Acad. Sci. U. S. A* 2013, 110, 19754–19759. [PubMed: 24248379]
23. Ayoub AM; Hawk LML; Herzig RJ; Jiang J; Wisniewski AJ; Gee CT; Zhao P; Zhu JY; Berndt N; Offei-Addo NK; Scott TG; Qi J; Bradner JE; Ward TR; Schonbrunn E; Georg GI; Pomerantz WCK BET bromodomain inhibitors with one-step synthesis discovered from virtual screen. *J. Med. Chem* 2017, 60, 4805–4817. [PubMed: 28535045]
24. Dawson M; Stein EM; Huntly BJP; Karadimitris A; Kamdar M; Fernandez de Larrea C; Dickinson MJ; Yeh PS-H; Daver N; Chaidos A; Tallman MS; Jiménez R; Horner T; Baron J; Brennan J; Ferron-Brady G; Wu Y; Karpinich N; Kremer B; Dhar A; Borthakur G A Phase I Study of GSK525762, a Selective Bromodomain (BRD) and Extra Terminal Protein (BET) Inhibitor: Results from Part 1 of Phase I/II Open Label Single Agent Study in Patients with Acute Myeloid Leukemia (AML). *Blood* 2017, 130, 1377–1377. [PubMed: 28667012]
25. Cousin S; Blay J-Y; Braña Garcia I; De Bono JS; Le Tourneau C; Moreno V; Trigo JM; Hann CL; Azad A; Im S-A; Ferron-Brady G; Datta A; Wu Y; Horner T; Kremer BE; Dhar A; O'Dwyer PJ; Shapiro G; Piha-Paul SA BET inhibitor molibresib for the treatment of advanced solid tumors: Final results from an open-label phase I/II study. *J. Clin. Oncol* 2020, 38, 3618–3618.
26. Tang P; Zhang J; Liu J; Chiang C-M; Ouyang L Targeting bromodomain and extraterminal proteins for drug discovery: From current progress to technological development. *J. Med. Chem* 2021, 64, 2419–2435. [PubMed: 33616410]
27. Sun Y; Han J; Wang Z; Li X; Sun Y; Hu Z Safety and Efficacy of Bromodomain and Extra-Terminal Inhibitors for the Treatment of Hematological Malignancies and Solid Tumors: A Systematic Study of Clinical Trials. *Front. Pharmacol* 2021, 11, 2440.
28. Faivre EJ; McDaniel KF; Albert DH; Mantena SR; Plotnik JP; Wilcox D; Zhang L; Bui MH; Sheppard GS; Wang L; Sehgal V; Lin X; Huang X; Lu X; Uziel T; Hessler P; Lam LT; Bellin RJ; Mehta G; Fidanze S; Pratt JK; Liu D; Hasvold LA; Sun C; Panchal SC; Nicolette JJ; Fossey SL; Park CH; Longenecker K; Bigelow L; Torrent M; Rosenberg SH; Kati WM; Shen Y Selective inhibition of the BD2 bromodomain of BET proteins in prostate cancer. *Nature* 2020, 578, 306–310. [PubMed: 31969702]
29. Gilan O; Rioja I; Knezevic K; Bell MJ; Yeung MM; Harker NR; Lam EYN; Chung C.-w.; Bamborough P; Petretich M; Urh M; Atkinson SJ; Bassil AK; Roberts EJ; Vassiliadis D; Burr ML; Preston AGS; Wellaway C; Werner T; Gray JR; Michon A-M; Gobbetti T; Kumar V; Soden PE; Haynes A; Vappiani J; Tough DF; Taylor S; Dawson S-J; Bantscheff M; Lindon M; Drewes G; Demont EH; Daniels DL; Grandi P; Prinjha RK; Dawson MA Selective targeting of BD1 and BD2 of the BET proteins in cancer and immunoinflammation. *Science* 2020, 368, 387. [PubMed: 32193360]
30. Tanaka M; Roberts JM; Seo HS; Souza A; Paulk J; Scott TG; DeAngelo SL; Dhe-Paganon S; Bradner JE Design and characterization of bivalent BET inhibitors. *Nat. Chem. Biol* 2016, 12, 1089–1096. [PubMed: 2775715]
31. Rathke C; Baarends WM; Awe S; Renkawitz-Pohl R Chromatin dynamics during spermiogenesis. *Biochim. Biophys. Acta* 2014, 1839, 155–168. [PubMed: 24091090]
32. Wang T; Gao H; Li W; Liu C Essential role of histone replacement and modifications in male fertility. *Front. Genet* 2019, 10, 962–962. [PubMed: 31649732]
33. Miao Z; Guan X; Jiang J; Georg GI, BRDT inhibitors for male contraceptive drug discovery: current status. In *Targeting Protein-Protein Interactions by Small Molecules*, Sheng C; Georg GI, Eds. Springer Singapore: 2018; pp 287–315.
34. Woods AS; Ferre S Amazing stability of the arginine-phosphate electrostatic interaction. *J. Proteome Res* 2005, 4, 1397–1402. [PubMed: 16083292]
35. Woods AS; Moyer SC; Jackson SN Amazing stability of phosphate-quaternary amine interactions. *J. Proteome Res* 2008, 7, 3423–3427. [PubMed: 18578519]

36. Cortopassi WA; Kumar K; Paton RS Cation- π interactions in CREBBP bromodomain inhibition: an electrostatic model for small-molecule binding affinity and selectivity. *Org. Biomol. Chem* 2016, 14, 10926–10938. [PubMed: 27814427]
37. Dougherty DA Cation- π interactions involving aromatic amino acids. *J. Nutr* 2007, 137, 1504S–1517S. [PubMed: 17513416]
38. Kumar K; Woo SM; Siu T; Cortopassi WA; Duarte F; Paton RS Cation- π interactions in protein-ligand binding: theory and data-mining reveal different roles for lysine and arginine. *Chem. Sci* 2018, 9, 2655–2665. [PubMed: 29719674]
39. Armstrong CT; Mason PE; Anderson JL; Dempsey CE Arginine side chain interactions and the role of arginine as a gating charge carrier in voltage sensitive ion channels. *Sci. Rep* 2016, 6, 21759. [PubMed: 26899474]
40. Kalra P; McGraw L; Kimbrough JR; Pandey AK; Solberg J; Cui H; Divakaran A; John K; Hawkinson JE; Pomerantz WCK Quantifying the selectivity of protein-protein and small molecule interactions with fluorinated tandem bromodomain reader proteins. *ACS Chem. Biol* 2020, 15, 3038–3049. [PubMed: 33138352]
41. Pauli GF; Chen SN; Simmler C; Lankin DC; Godecke T; Jaki BU; Friesen JB; McAlpine JB; Napolitano JG Correction to importance of purity evaluation and the potential of quantitative (^1H) NMR as a purity assay. *J. Med. Chem* 2015, 58, 9061. [PubMed: 26602703]
42. Pauli GF; Chen SN; Simmler C; Lankin DC; Godecke T; Jaki BU; Friesen JB; McAlpine JB; Napolitano JG Importance of purity evaluation and the potential of quantitative (^1H) NMR as a purity assay. *J. Med. Chem* 2014, 57, 9220–9231. [PubMed: 25295852]
43. Elzein E; Kalla RV; Li X; Perry T; Gimbel A; Zeng D; Lustig D; Leung K; Zablocki J Discovery of a novel A2B adenosine receptor antagonist as a clinical candidate for chronic inflammatory airway diseases. *J. Med. Chem* 2008, 51, 2267–2278. [PubMed: 18321039]
44. Ember SW; Zhu JY; Olesen SH; Martin MP; Becker A; Berndt N; Georg GI; Schonbrunn E Acetyl-lysine binding site of bromodomain-containing protein 4 (BRD4) interacts with diverse kinase inhibitors. *ACS Chem. Biol* 2014, 9, 1160–1171. [PubMed: 24568369]
45. Kabsch W Xds. *Acta Crystallogr. Sect. D. Biol. Crystallogr* 2010, 66, 125–132. [PubMed: 20124692]
46. Adams PD; Afonine PV; Bunkoczi G; Chen VB; Davis IW; Echols N; Headd JJ; Hung LW; Kapral GJ; Grosse-Kunstleve RW; McCoy AJ; Moriarty NW; Oeffner R; Read RJ; Richardson DC; Richardson JS; Terwilliger TC; Zwart PH PHENIX: a comprehensive Python-based system for macromolecular structure solution. *Acta Crystallogr. Sect. D. Biol. Crystallogr* 2010, 66, 213–221. [PubMed: 20124702]
47. Emsley P; Lohkamp B; Scott WG; Cowtan K Features and development of Coot. *Acta Crystallogr. Sect. D. Biol. Crystallogr* 2010, 66, 486–501. [PubMed: 20383002]
48. Chen VB; Arendall WB 3rd; Headd JJ; Keedy DA; Immormino RM; Kapral GJ; Murray LW; Richardson JS; Richardson DC MolProbity: all-atom structure validation for macromolecular crystallography. *Acta Crystallogr. Sect. D. Biol. Crystallogr* 2010, 66, 12–21. [PubMed: 20057044]
49. Afonine PV; Grosse-Kunstleve RW; Chen VB; Headd JJ; Moriarty NW; Richardson JS; Richardson DC; Urzhumtsev A; Zwart PH; Adams PD phenix.model_vs_data: a high-level tool for the calculation of crystallographic model and data statistics. *J. Appl. Crystallogr* 2010, 43, 669–676. [PubMed: 20648263]
50. Stierand K; Maass PC; Rarey M Molecular complexes at a glance: automated generation of two-dimensional complex diagrams. *Bioinformatics* 2006, 22, 1710–1716. [PubMed: 16632493]

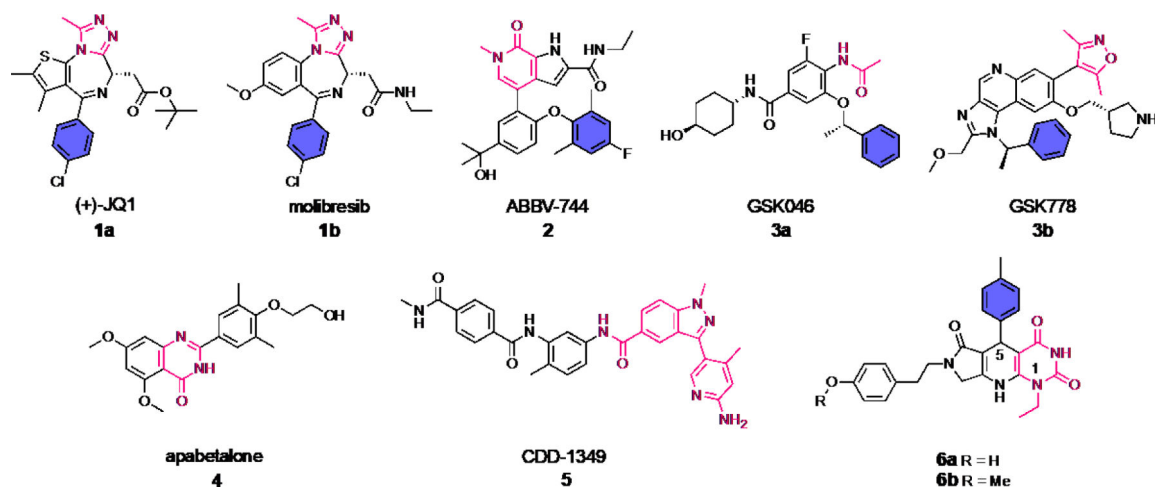


Figure 1.
Structures of representative BET inhibitors. The acetylated lysine mimic is highlighted in pink and the moiety that occupies the WPF shelf is marked in blue.

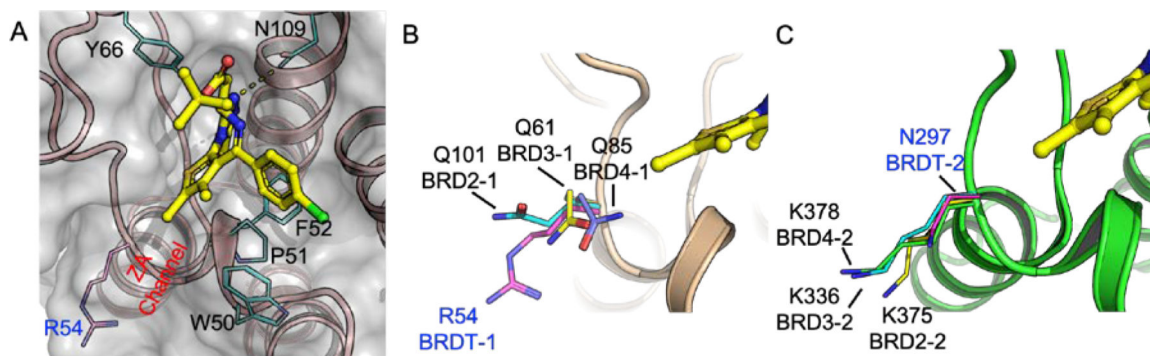


Figure 2.

Binding mode of (+)-JQ1 and the sequence analysis of the BD1 bromodomains of the BET family. (A) The surface view of (+)-JQ1/BRDT-1 complex (PDB ID: 4FLP). The key residues are highlighted in cyan sticks, the key hydrogen bond is highlighted in yellow dashes. The R54 side chain is shown in magenta. (B) The superimposition of four BD1 bromodomains in the BET family. One major difference around the recognition site lies in the ZA channel, in which BRDT-1 (PDB ID: 4FLP) has a positively charged arginine (magenta), whereas BRD2-1, BRD3-1, and BRD4-1 (PDB IDs: 6DDI, 6QJU, and 5KDH) have neutral glutamines (highlighted in cyan, yellow, and purple, respectively). (C) The sequence difference among four BD2 bromodomains. BRDT-2 (PDB ID: 2WP1) has an asparagine (magenta), whereas BRD2-2, BRD3-2, and BRD4-2 (PDB IDs: 5XHK, 5A7C, and 6DUV) have lysines (highlighted in yellow, cyan, and green, respectively).

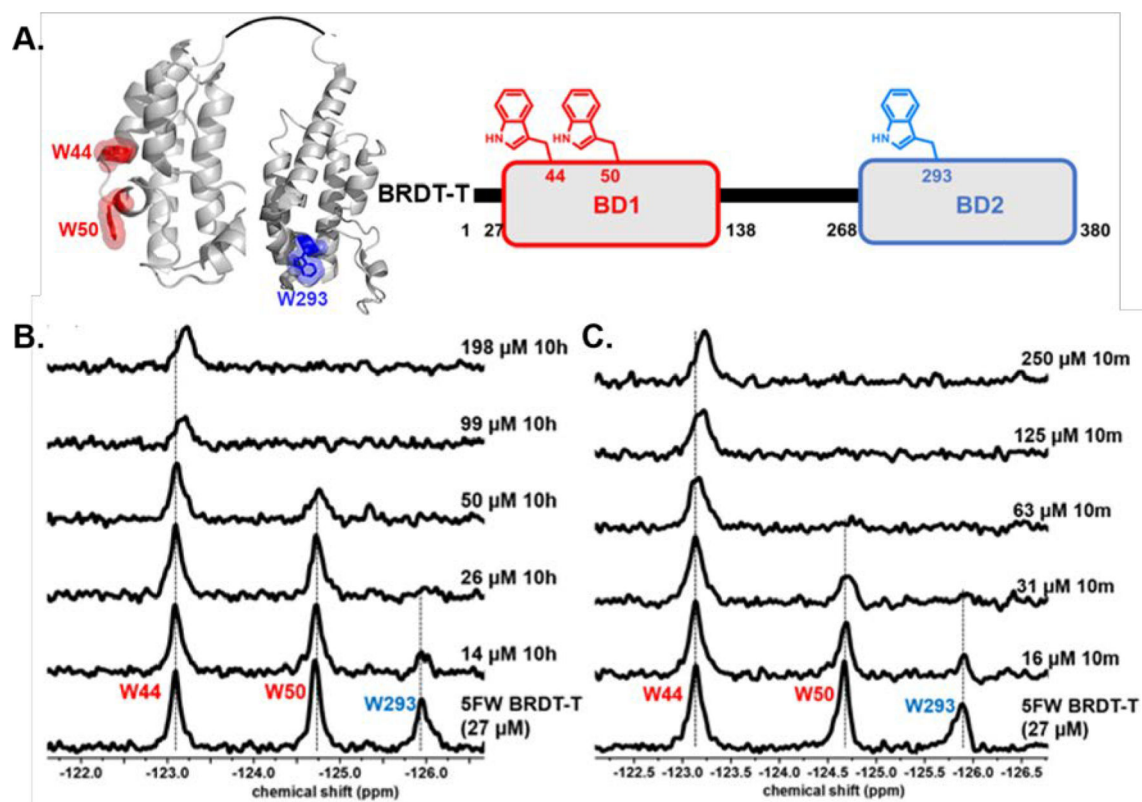


Figure 3.

PrOF NMR experiments of **10h** and **10m** with 5FW BRDT-T. (A) BD1 and BD2 crystal structures in BRDT Tandem (BRDT-T) and schematic of the domain architecture. Stacked ¹⁹F NMR spectra with an increasing concentration of (B) **10h** and (C) **10m** with 27 μM 5FW BRDT-T. W50 and W293 are the WPF shelf tryptophans in BD1 and BD2 of BRDT-T, colored red and blue, respectively.

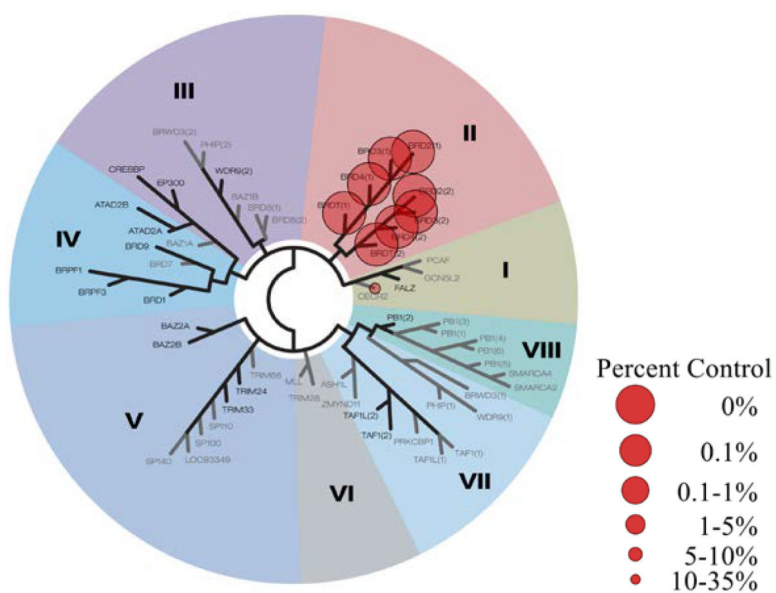


Figure 4. Selectivity of **10 m** at 20 μ M concentration against a panel of 33 bromodomains. BET bromodomains are in bromodomain family II.

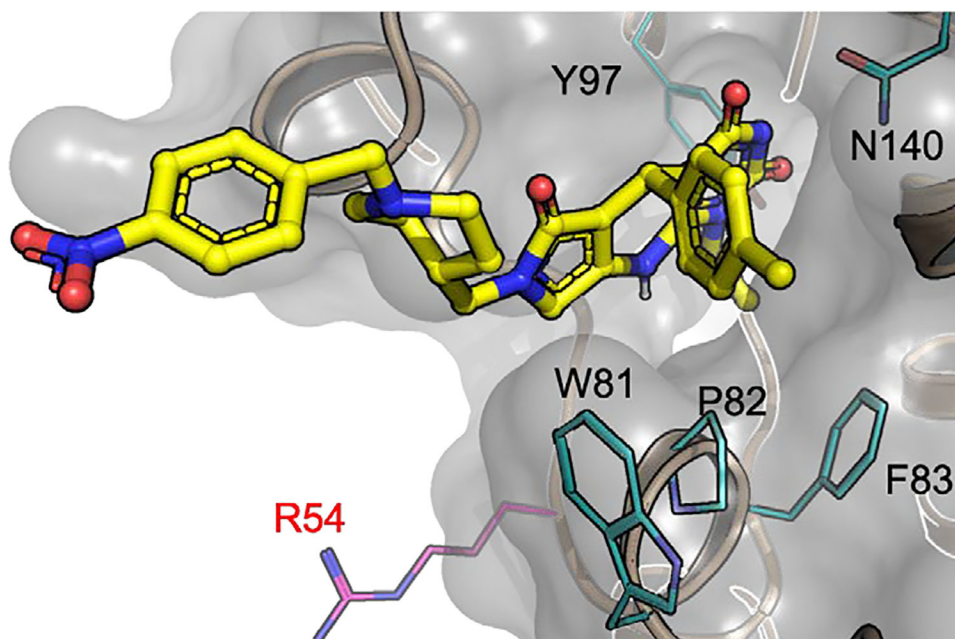
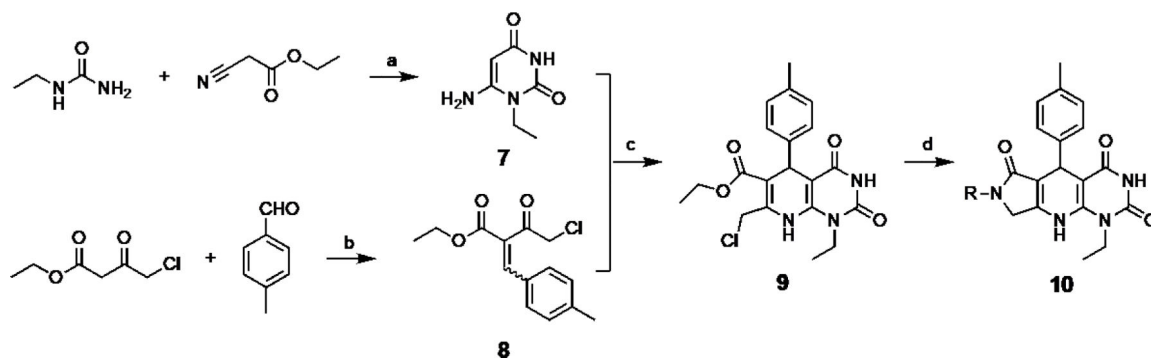
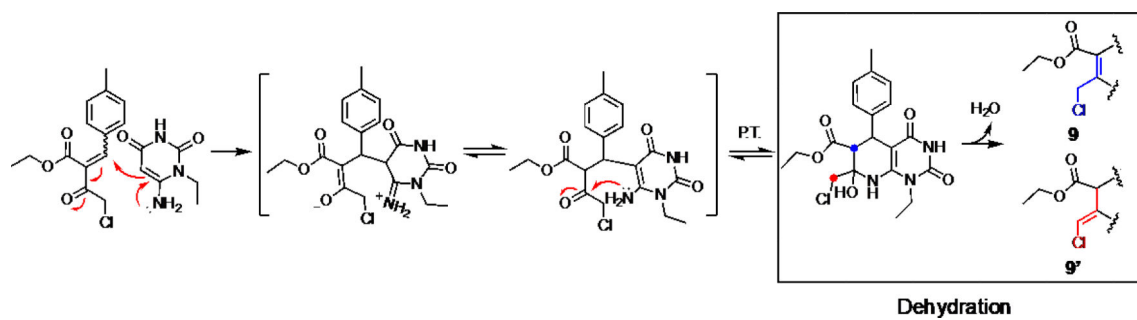


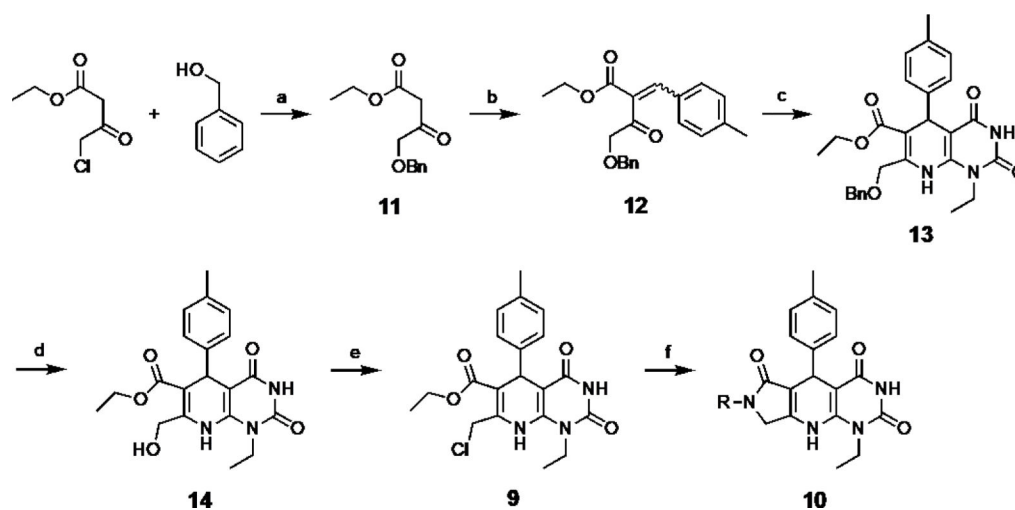
Figure 5. Binding conformation of nitro compound **10j** (yellow) in the KAc binding site of BRD4-1 (PDB ID: 7LH8). In this co-crystal structure, the lactam side chain is solvent exposed. A superimposition with BRDT-1 (PDB ID: 4FLP) revealed that the lactam side chain is spatially distant from the target R54 (R54 highlighted in magenta).

**Scheme 1.**

Initial route for the lactam analogs. *Reagents and conditions:* a) sodium *tert*-butoxide (2 equiv), ethanol, reflux, 91%; b) piperidine (0.1 equiv), ethanol, 25 °C, 57%; c) magnesium sulfate, methanol, 45 °C, 14%; d) primary amine (1.2 equiv), ethanol, microwave to 120 °C.

**Scheme 2.**


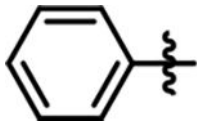
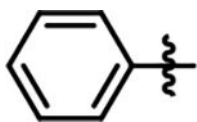
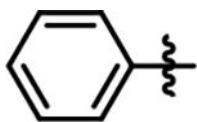
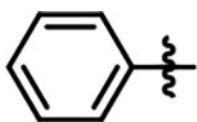
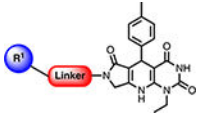
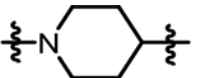
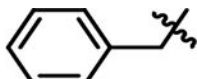
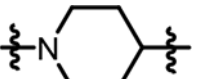
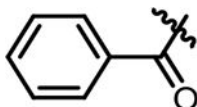
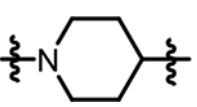
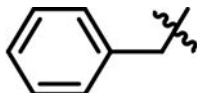
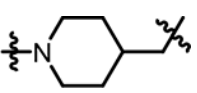
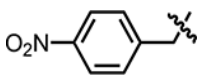
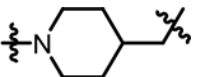
Proposed mechanism for the Hantzsch dihydropyridine formation. The electron transfers are rendered in red curved arrows. The dehydration step in the box could generate target molecule **9** (at the carbon highlighted by a blue dot) and regioisomer **9'** (at the carbon highlighted by a red dot).

**Scheme 3.**

Optimized route for the synthesis of lactam analogs. *Reagents and conditions:* a) sodium hydride (2.2 equiv), ethanol, 0 °C to 25 °C, 96%; b) piperidine (0.1 equiv), ethanol, 25 °C, 56%; c) uracil **7** (1.0 equiv), acetic acid, reflux, 42%; d) 1 M boron tribromide solution in THF (2.2 equiv), dichloromethane, -78 °C, 58%; e) sulfuric acid (1.2 equiv), imidazole (2.2 equiv), DMF, 0 °C to 25 °C, 56%; f) primary amine (1.2 equiv), ethanol, microwave to 120 °C, 10–45%.

Table 1.

Structure and Inhibitory Profile of 1st Round Modifications

Compound Number	R ¹	Linker	IC ₅₀ (μM) BRDT-1	IC ₅₀ (μM) BRDT-2	IC ₅₀ (μM) BRD4-1	IC ₅₀ (μM) BRD4-2
10a		-CH ₂ -	1.3±0.39	0.70±0.07	1.3±0.21	1.1±0.06
10b		-CH ₂ -	2.6±0.69	0.56±0.09	0.90±0.11	0.60±0.05
10c		-C ₂ H ₄ -	7.6±1.7	1.2±0.12	2.3±0.48	1.4±0.12
10d		-C ₃ H ₆ -	15±6.8	1.8±0.32	4.9±1.5	2.9±0.48
10e	 	-OC ₂ H ₄ -	8.1±1.8	0.84±0.16	2.0±0.83	1.2±0.148
10f	Me		4.9±0.41	1.1±0.11	2.5±0.30	2.1±0.11
10g			8.0±0.73	1.5±0.22	2.9±0.28	2.3±0.15
10h			13±2.7	0.89±0.09	2.1±0.49	1.8±0.16
10i			5.0±1.09	0.57±0.05	1.4±0.20	1.1±0.06
10j			2.8±0.47	0.64±0.05	1.1±0.12	1.0±0.05

Compound Number	R ¹	Linker	IC ₅₀ (μM) BRDT-1	IC ₅₀ (μM) BRDT-2	IC ₅₀ (μM) BRD4-1	IC ₅₀ (μM) BRD4-2
(+)-JQ1 *	-	-	1.0±0.1	1.1±0.8	0.37±0.1	0.30±0.01

* (+)-JQ1 was used as the positive control in the AlphaScreen assay. All compounds were tested in quadruplicate. The ± indicates standard deviation.

Author Manuscript

Author Manuscript

Author Manuscript

Author Manuscript

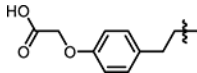
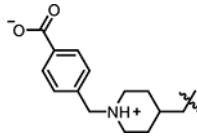
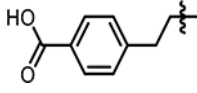
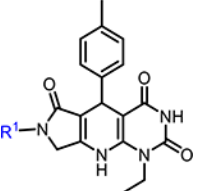
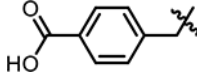
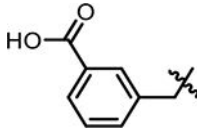
Table 2.Structure and Inhibitory Profile of 2nd Round Modifications

Compound Number	R ¹	IC ₅₀ (μM) BRDT-1	IC ₅₀ (μM) BRDT-2	IC ₅₀ (μM) BRD4-1	IC ₅₀ (μM) BRD4-2
10c	H	7.6±1.7	1.2±0.08	2.3±0.48	1.4±0.12
10k	4-Me	12±1.9	2.2±0.07	3.5±0.93	2.1±0.16
10l	4-Cl	25±4.1	3.1±0.24	6.3±2.1	3.0±0.49
6a	4-OH	2.2±0.76	0.61±0.06	1.3±0.20	0.82±0.03
6b	4-OMe	4.3±0.26	104±13	0.60±0.15	0.98±0.04
10m	3-OMe	18±3.6	1.2±0.08	1.9±0.42	1.3±0.09
10n	2-OMe	9.4±1.1	1.5±0.07	2.3±0.40	1.6±0.08
10o	3,4-diOMe	103±12	14±2	23±0.79	17±2.84
10p	2,3-diOMe	69±8.7	13±2.8	20±1.2	11±3.5
10q	3,4-diCl	35±3.64	8.4±1.7	13±3.8	6.0±1.5
(+)-JQ1 [*]	-	1.0±0.1	1.1±0.8	0.37±0.1	0.30±0.01

^{*}(+)-JQ1 was used as the positive control in the AlphaScreen assay. All compounds were tested in quadruplicate. The ± indicates standard deviation.

Table 3.

Structure and Inhibitory Profile of 3rd Round Modifications

Compound Number	R ¹	IC ₅₀ (μM) BRDT-1	IC ₅₀ (μM) BRDT-2	IC ₅₀ (μM) BRD4-1	IC ₅₀ (μM) BRD4-2	
10r		18±2.1	2.9±0.13	4.0±0.96	3.1±0.25	
10s		6.7±0.65	1.2±0.06	0.85±0.09	1.3±0.08	
10t	 	7.3±0.73	1.2±0.05	0.98±0.12	1.1±0.07	
10u		5.8±0.66	1.1±0.05	0.94±0.08	1.2±0.08	
10v		3.1±0.15	41±3.2	0.42±0.11	0.97±0.04	
(+)-JQ1*	-	-	1.0±0.1	1.1±0.8	0.37±0.1	0.30±0.01

* (+)-JQ1 was used as the positive control in the AlphaScreen assay. All compounds were tested once in quadruplicate. The ± indicates standard deviation.